# DEVELOPMENT AND EXPERIMENTAL CHARACTERIZATION OF FILAMENT WOUND HYBRID CYLINDIRICAL STRUCTURES WITH ENHANCED THERMAL PROPERTIES

**A Thesis Submitted to**
**the Graduate School of Engineering and Sciences of**
**Izmir Institute of Technology**
**in Partial Fulfillment of the Requirements for the Degree of**

**MASTER OF SCIENCE**

**in Mechanical Engineering**

**by**
**Dora ÖZARSLAN**

**June 2023**
**İZMİR**

We approve the thesis of **Dora ÖZARSLAN**

**Examining Committee Members:**

**Prof. Dr. Metin TANOĞLU**

Department of Mechanical Engineering, İzmir Institute of Technology

**Prof. Dr. Engin AKTAŞ**

Department of Civil Engineering, İzmir Institute of Technology

**Doç. Dr. Aylin ZİYLAN**

Department of Metallurgical and Materials Engineering, Dokuz Eylül University

**19 June 2023**

**Prof. Dr. Metin TANOĞLU**

Supervisor, Department of Mechanical Engineering, İzmir Institute of Technology

**Prof. Dr. Metin TANOĞLU**

Department of Mechanical Engineering, İzmir Institute of Technology

**Prof. Dr. Mehtap EANES**

Dean of the Graduate School of Engineering and Science

# ACKNOWLEDGMENTS

I would like to sincerely thank my thesis advisor, Prof. Dr. Metin TANOĞLU for his guidance and support through the learning and writing processes of my master thesis.

I am deeply grateful and like to thank my laboratory colleague, my friend Seçkin MARTİN for sharing his knowledge, invaluable contributions, patience, and encouragements.

I would like to also thank Yusuf Can UZ and Prof. Dr. Aref CEVAHİR for their help and advice on the subject.

I am especially grateful for my colleague Mert ÖZKAN for his support and assistance during this thesis.

I am grateful for my laboratory colleagues, my friends Ahmet Ayberk UÇKUN, Ceren TÜRKDOĞAN, Kaan NUHOĞLU, Melisa YEKE, Muhammed Erdal ULAŞLI and Nazife Çerçi for their support and motivation through this process.

Finally, I must express my deep gratitude to my family and for providing me with endless support and continuous encouragement through the process of my education and writing this thesis. Without them, this accomplishment would not have been possible.

# ABSTRACT


## DEVELOPMENT AND EXPERIMENTAL CHARACTERIZATION OF FILAMENT WOUND HYBRID CYLINDRICAL STRUCTURES WITH ENHANCED THERMAL PROPERTIES

Composite tube components have key roles in many industrial applications, such as pipelines, drive shafts, airplane fuselages, and offshore construction components. Filament winding technology has enabled precise tailoring and manufacturing processes, allowing for a variety of applications to be manufactured with advanced machinery.

In this study, the aim was to enhance the thermal properties without any significant change in the mechanical properties. Therefore, the samples were manufactured as carbon fiber composite tubes with different resin layer configurations by utilizing filament winding technology. The fiber orientation was set to a 55° winding angle with a 5/3 pattern to wrap over a 58.8 mm diameter mandrel as a 5-layer stacking. Due to difficulties in manufacturing different stacked groups of phenolin resin layers, only two groups (one with a 5-layer carbon epoxy resin group and one with a 4-layer carbon epoxy resin with 1 outer layer of carbon phenolin resin group) were successfully manufactured and thus tested. For each group, with dimensions of ±62.7 mm outer diameter and ±1.95 mm thickness with an 800 mm length, two composite tubes were manufactured. Before the test procedures, the homogeneity and quality of the groups were analyzed.

For the observation of properties, mechanical and thermal tests were conducted: Apparent hoop tensile, radial compression, 3-point bending, Flammability, Thermogravimetric analysis, Differential scanning calorimeter, Thermal conductivity. The tests were proceeded according to their standards.

The results and failure behaviors demonstrate that, with the replacement of the outer layer with phenolin resin, no significant improvement or drawback was observed compared to its fully epoxy resin counterpart.

# ÖZET


## GELİŞTİRİLMİŞ TERMAL ÖZELLİKLERE SAHİP FİLAMAN SARGILI HİBRİT SİLİNDİRİK YAPILARIN GELİŞTİRİLMESİ VE DENEYSEL KARAKTERİZASYONU

Kompozit boru bileşenleri, boru hatları, tahrik milleri, uçak gövdesi ve açık deniz inşaat bileşenleri gibi birçok endüstriyel uygulamada kilit rollere sahiptir. Filament sarma teknolojisi, hassas terzilik ve üretim süreçlerini mümkün kılarak, gelişmiş makinelerle çeşitli uygulamaların üretilmesine olanak sağlamıştır.

Bu çalışmada amaç, mekanik özelliklerde önemli bir değişiklik olmaksızın termal özelliklerin arttırılmasıdır. Bu nedenle numuneler, filament sarma teknolojisi kullanılarak farklı reçine tabaka konfigürasyonuna sahip karbon fiber kompozit tüpler olarak üretilmiştir. Fiber oryantasyonu, 58,8 mm çapında bir mandrel üzerine 5 katmanlı istifleme olarak sarılması için 55° sarım açısına ayarlandı. Farklı istiflenmiş fenolin reçine tabaka gruplarının üretilmesinin zorlukları nedeniyle, biri 5 katmanlı karbon epoksi reçine grubu, diğeri 4 katmanlı karbon-epoksi reçinesi ve 1 (dış) tabakalı karbon-fenolin reçine grubu olan sadece iki grup başarıyla üretildi ve böylece test edildi. Her grup için ±62.7 mm dış çap ve ±1.95 mm kalınlık ölçülerinde 800mm uzunluğunda iki kompozit boru imalatı yapılmıştır. Test prosedürlerinden önce grupların homojenliği ve kalitesi analiz edilmiştir.

Özelliklerin gözlemlenmesi için mekanik ve termal testler yapıldı: Görünür çember çekme; Radyal basma; 3-nokta eğme; Alevlenebilirlik; Termogravimetrik analiz; Diferansiyel taramalı kalorimetre; Isı iletkenliği. Testler standartlara uygun olarak yapılmıştır.

Sonuçlar ve kırılma davranışları, dış tabakanın fenolin reçinesi olarak değiştirilmesiyle, tamamen epoksi reçine muadili ile karşılaştırıldığında kayda değer herhangi bir iyileşme veya dezavantaj gözlenmediğini göstermektedir.

# TABLE OF CONTENTS

# LIST OF FIGURES

**Figure** **Page**

**Figure** **Page**

**Figure** **Page**

# LIST OF TABLES

**Table** **Page**

# CHAPTER 1

# INTRODUCTION

From the beginning of humanity, the search for better materials has always been one of the key elements of technological advancement. Therefore, there are numerous experiments, from basic parameters to complex reaction processes, to obtain the best or ideal material for specific applications. In this chapter, utilized materials and manufacturing techniques will be explained briefly.

## 1.1 Introduction of Composite Materials

The composite material terminology has been used since ancient times because of the advantages of material combinations. From humanity to nature, numerous examples of use can be given. Such as birds using various materials to build a nest, and for the same purpose, humans also built homes with straw and clay combinations. A similar application can be given as a simple example of today's technology, like buildings with steel and concrete structures. [1]

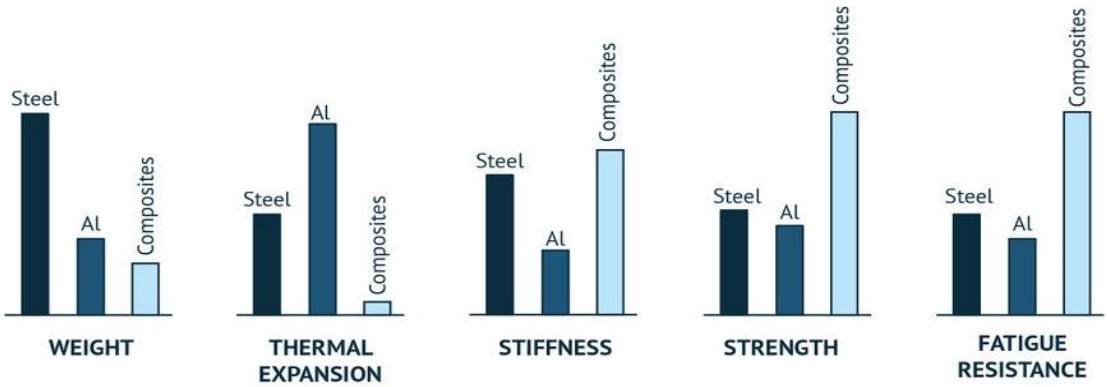


Figure 1.1. Comparison of properties of composite and common industrial materials [2]

Due to these examples, a composite material can be defined as the combination or dispersion of one or more types of reinforcement components within the matrix material, which is the base filler structure of a chemical or physical corporation. The final product results in a combination of superior properties of each component with desired properties

or optimized performance. These properties are unobtainable by using monolithic materials. Specific or optimized properties can be obtained by changing the component parameters, such as the volume fraction, the size of particles or fibers, distribution, or configuration in the matrix. [1]

The phases of components can be of several types, such as nanoparticles to liquid reinforcement materials. As seen in many examples in the industry, due to their strength and stiffness, fibers are the most common type of reinforcement for advanced composites. Depending on the manufacturing process, fibers can be either continuous or discontinuous. Composite materials play a significant role in engineering materials due to their superior properties compared to common industrial materials, as shown below in Figure 1.1. [1] [2]

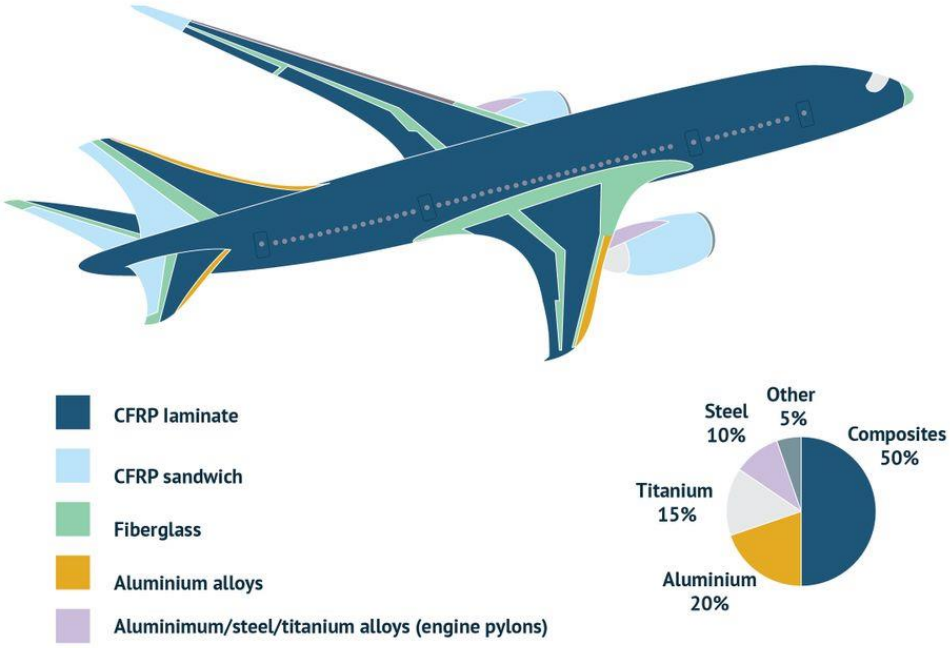


Figure 1.2. Distribution of materials used in the Boeing 787 (2017) [2]

When strength and stiffness are considered alone, it may not be beneficial to use composite materials compared to metals or such, but the main benefit comes from the strength-weight or modulus-weight ratio of composites. Therefore, composites are crucial for specific weight reduction applications, such as the transportation industry, as shown in Figure 1.2. [1] [3]

## 1.2. Composite Material Processing Methods

Besides their properties, the composites are significantly different in the way they are manufactured. Conventional metalworking methods like casting and machining are not applicable. On the other hand, there are numerous options for fabricating composites, depending on the form. As shown in Figure 1.3, these manufacturing methods are not applicable to every composite material. [3]

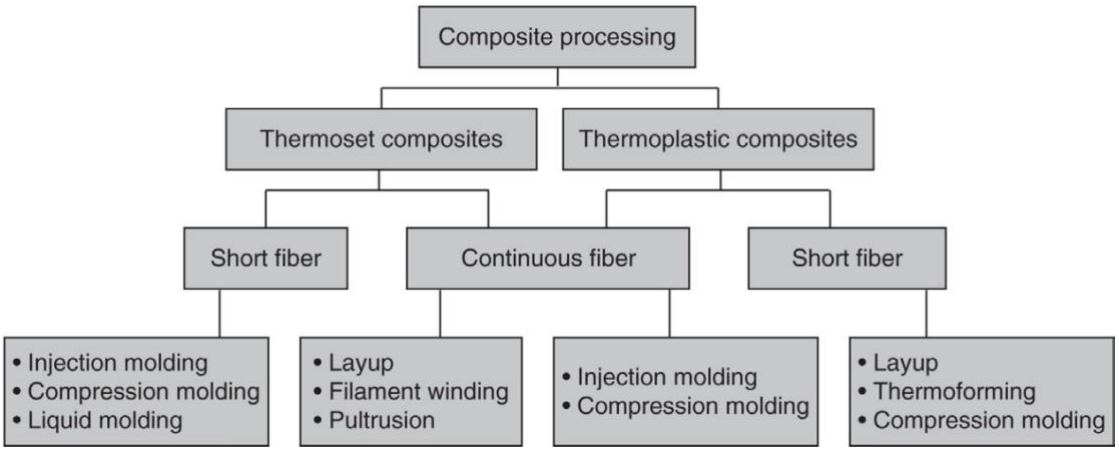


Figure 1.3. Composite material processing methods [3]

Since in this study only the filament winding method was utilized with carbon fiber, which is a continuous fiber type, to manufacture composite tubes, other methodologies were not detailed.

### 1.2.1. Filament Winding Process

The filament winding technology is a composite manufacturing technique with an elevated level of quality and automation that has changed the production of cylindrical composite structures in various areas, especially gas storage and transportation.

In this technique, the fiber filaments are wound continuously on a rotating mandrel or different type of shape under tension to create a hollow structure in a predetermined orientation. With precise automation, filament winding is also beneficial for mass production. [4] [5]

For a variety of applications, the filament winding approach is mostly used with axisymmetric structures, such as drive shafts, fishing rods, pressure vessels, missile cases,

bicycle components, and airplane fuselages. With the advances of technology and the ability to use multiple axis windings, axial asymmetrical geometries can also be produced. [4] [5]

Figure 1.4. Filament winding axisymmetric examples (Source: Mateduc Composites)

Basic winding machines use mandrel rotation and carriage travel (typically horizontal) as the two axes of motion. Pipe manufacturing is the sole use for two-axis machines. A four-axis winding machine is necessary for pressure vessels, such as gas storage tanks. A rotating fiber payout head positioned on the cross-feed axis and an additional radial (cross-feed) axis parallel to carriage movement are features of the four-axis machine. [4] [7]

Machines with four or more axes can be utilized to create complex structures. The six-axis winding machines generally have three linear and three rotation axes. Such machines with more than two axes of motion require computer control, which is provided with the help of suitable software to generate the winding patterns and machine paths. Therefore, complex shapes can be manufactured with high quality, reliability, and repeatability. To prevent the fiber band from twisting and fluctuating in width while being wound, payout head rotation can be used. [4] [7]

The fiber placement is guided by a machine with two or more axes of motion. It is possible to manufacture several types of components using a variety of different filament winding machine designs. The winding of the fibers can be configured in a precise pattern by using the software to configure machine paths that are suitable for the selected axis-machine setup.

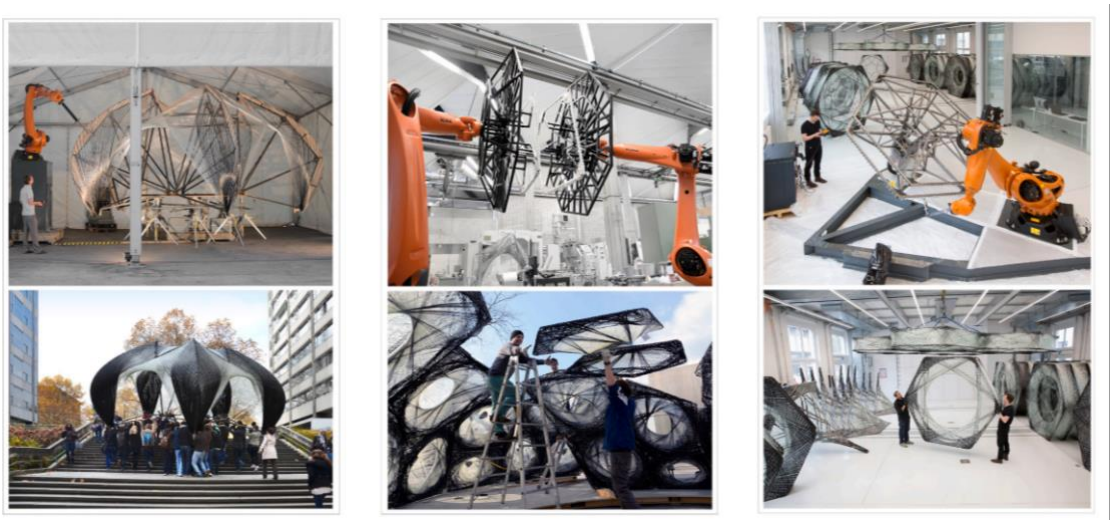

Figure 1.5. Complex coreless filament winding in construction process and end-product examples [6]

To tailor the product's desired end quality, optimization of resin type, fiber type, fiber tension, winding thickness, winding angle, speed, etc. is necessary. These parameters require software and a suitable machine to be configured.

For high-angle winding, tension is an essential component of the winding process. Fiber volume fraction, void content, and the strength or stiffness of the part are all directly impacted by fiber tension. In other words, improved fiber compaction made possible by higher fiber tension provides fiber volume fraction management. These configurations can also be analyzed in simulation before the manufacturing process to verify repeatability and quality. [4]

Figure 1.6 shows the schematic setup and general layout of the filament winding technique. Each component can vary depending on the complexity of the machine and application.

In the winding process, a stationary mandrel rotates while a carriage arm moves horizontally. Before wrapping around the mandrel, the fibers are impregnated with resin by being pulled through a resin bath. The winding pay-out eye on the arm gathers and dispenses with pre-impregnated fibers from roving of carbon fiber yarn, as an example. The fibers wrap around the mandrel as it rotates, creating a composite winding structure over the mandrel's surface. The precise direction of the composite winding depends on the carriage rate and the mandrel's rotational speed.

Following the completion of the fiber winding process, the composite structure with mandrel is placed in the oven to be heated to the necessary temperatures for curing.

When the composite resin is fully hardened (cured), the mandrel is removed, obtaining the final product as a hollow composite structure. [4]

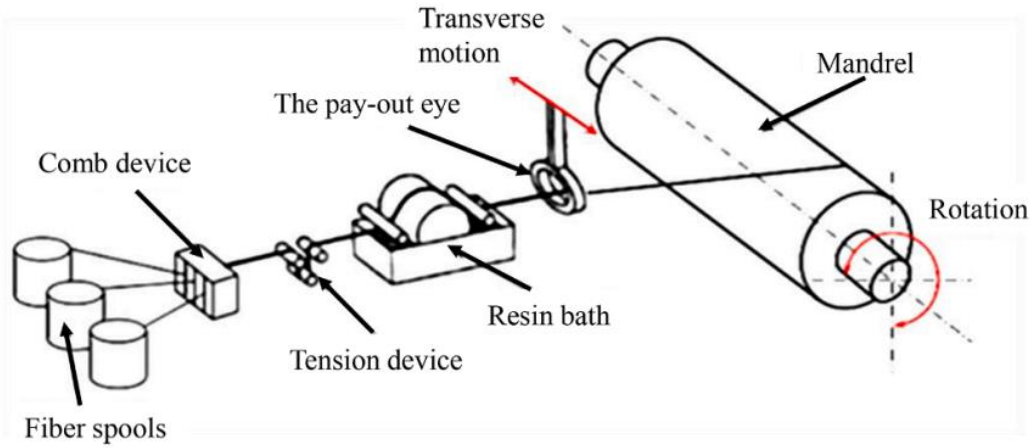


Figure 1.6. Filament winding setup schematics [4]

For the resin impregnation, there are two methods: wet and prepreg winding. Wet winding requires wrapping the fibers in the rotating mandrel after passing the fibers through a resin bath. For the prepreg winding, pre-impregnated fiber tows can be used without any further resin bath process directly to wind on the rotating mandrel with tension. Compared to wet winding, prepregs provide superior quality control, reliability, repeatability of resin content, bandwidth, and uniformity. [8]

A winding pattern can be either helical, polar, or circumferential. In helical winding, the fiber feed carriage moves rapidly back and forth while the mandrel rotates at a constant speed to create the necessary helix winding angle. An almost 90-degree helical winding angle characterizes the circumferential winding.

During the polar winding, the mandrel arm rotates around the longitudinal axis, and fibers are wound from pole to pole. [8]

The main advantages of filament winding can be listed as follows: Because of the automation, it can be a very quick and cost-effective process that provides low labor costs. The resin content can be controlled by measuring the resin on each fiber tow through clamps or dies. The fiber cost can be reduced because there is no additional process required to turn the fiber into fabric prior to use, and the laminate's structural properties can be excellent because straight fibers can be laid in a complex pattern to match the applied loads. [9] [10]

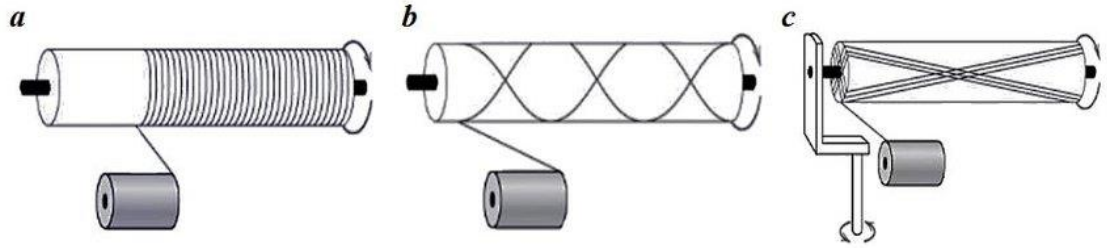


Figure 1.7. Winding types: a) Circumferential winding, b) Helical winding, c) Polar winding [8]

Despite the many advantages of filament winding, there are also significant disadvantages in several ways. Component geometry is limited and not capable of manufacturing concave-shaped products. Fiber cannot easily be laid exactly along the length of a component. Equipment and maintenance costs can be high, especially for large components. Since the component's outer surface is unmolded, low surface quality may be cosmetically undesirable. Low-viscosity resins usually require auxiliary components, which reduces their mechanical properties. Because of automation, heavy machinery, and chemical processes, there is a risk to health and safety. [9] [10]

All the filament winding method's benefits, drawbacks, risks, and capability characteristics were considered in this study, and all necessary safety precautions were taken. In terms of filament winding production, the helical winding method has been used.

# CHAPTER 2

# LITERATURE REVIEW

With the development of filament winding technology, cylindrical structure production with composite materials has improved rapidly. Over time and with technological advancements, utilizing multiple-axis machinery and computer-aided systems made it possible to create such complex shapes, from simple pipelines to big, complex, coreless construction structures. This development requires optimization or tailoring for desired properties in specific applications. Therefore, many academic studies have been carried out to create better solutions or improve what has already been achieved. From optimizing base manufacturing parameters to creating different, even organic, material components, numerous research and experiments have been conducted.

In this chapter, some of the literature research that was investigated prior to this study to obtain extensive information will be investigated to demonstrate apparent, satisfying, and more organized research.

For the filament winding process, winding angle, wall thickness, and winding pattern are crucial factors in tailoring a reliable structure with the desired properties. The impact of filament winding parameters on the mechanical behavior of structures has been investigated in several studies. In this regard, Krishnan [11] and associates evaluated the effect of the winding angle on composite tubes under multiaxial pressure loadings in cycles. According to this investigation, the failure envelopes (maximum shear stress) revealed a significant relationship between stress ratio and winding angle. With a ±45° winding angle, indicating a tendency toward axial superiority, and a ±63° degree performing better under high hoop-dominant loads. Almeida Jr. [12] and associates designed an optimization method that utilized a genetic algorithm to calculate the ideal stacking order in composite tubes subjected to internal pressure loading. They discovered that for internally pressured tubes, asymmetrical and unusual angles increase their rupture strength.

The processing characteristics of epoxy composite tubes with two distinct epoxy resin systems, five different fiber types, and five different winding angles were examined by Kaynak [13] and his colleagues. The impacts of resin type, fiber type, and winding angle were thus investigated. To measure the hoop tensile strength and modulus of the

specimens, the split-disk test was utilized. They discovered that while using different epoxy resin systems had no appreciable effects, using carbon fibers instead of glass fibers and winding angles greater than 60° significantly improved the performance of the structures. Additionally, it has been found that split-disk tests are effective for evaluating the performance of tubular structures.

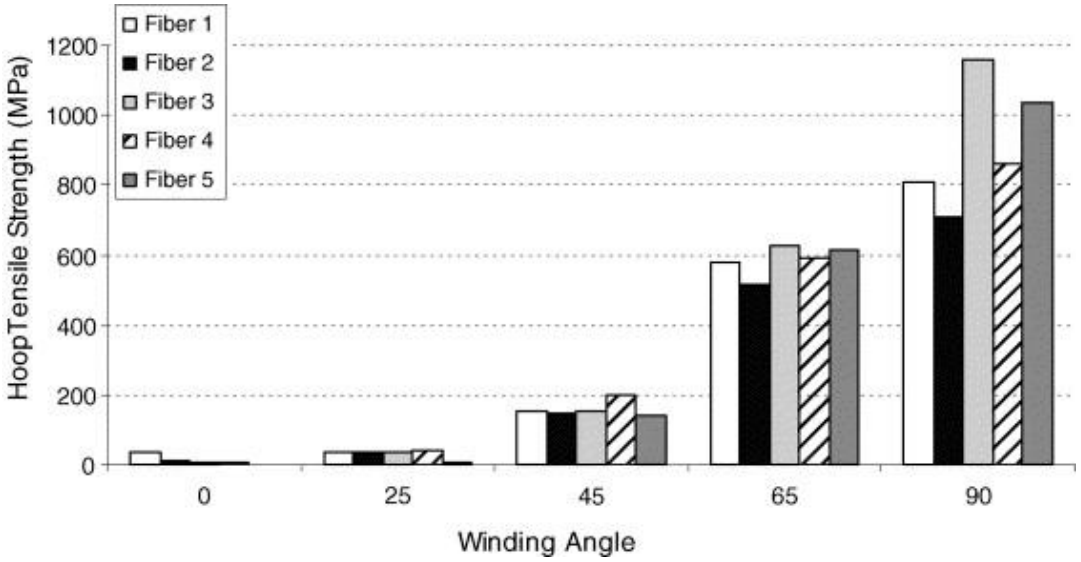


Figure 2.1. Comparison of hoop tensile strengths of specimens [13]

Morozov's [14] investigation of the impact of the winding pattern on tubes tested for internal pressure is one of the studies in the literature that deals with winding pattern modeling. As a result of the winding pattern being sensitive to the stress fields, the stresses were underestimated by conventional models that used nominal angles. The evaluation clarified that the winding pattern should not be underestimated in calculations and should be considered according to application. In another research, Morozov [15] and his associates also demonstrated the same results with finite element analysis by characterizing a filament wound spinning composite disk with the helically wound layers, which consist of curved triangular-shaped units alternating in the radial and circumferential directions.

The effects of filament winding parameters have been investigated many times for not only the tubes or pipes but also for the pressure vessels. Azeem [4] and associates reviewed the effects of filament winding on pressure vessels. They indicated that choosing an effective winding angle, fiber tension, and winding speed are crucial elements affecting the structure's effectiveness and quality. Additionally, a natural result

of filament winding technology is mosaic patterns. They also pointed out that asymmetrical parts can also be manufactured effectively. Thus, for applications in aerospace, shipping, medicine, and other fields, this method offers the best fiber-to-matrix ratio.

Due to the capability of filament winding, many research studies on hybrid composite structures with different application purposes were also conducted. Cui [16] and colleagues studied the crushing characteristics and failure mechanisms of multiple filament-winding hybrid tubes. Their results demonstrated that continuous brittle cracks, delamination modes in CFRP layers, and diamond failure modes in aluminum tubes were the dominant failure modes of hybrid specimens. Increasing hybrid plies increased the specific energy absorption, energy absorption, and peak crushing force. The peak crushing force of the hybrid tubes decreased with increasing CFRP winding angles from 30° to 60°, while the hybrid tubes with a winding angle of 45° showed the highest specific energy absorption and energy absorption. They concluded that interactions between various materials can significantly improve energy absorption.

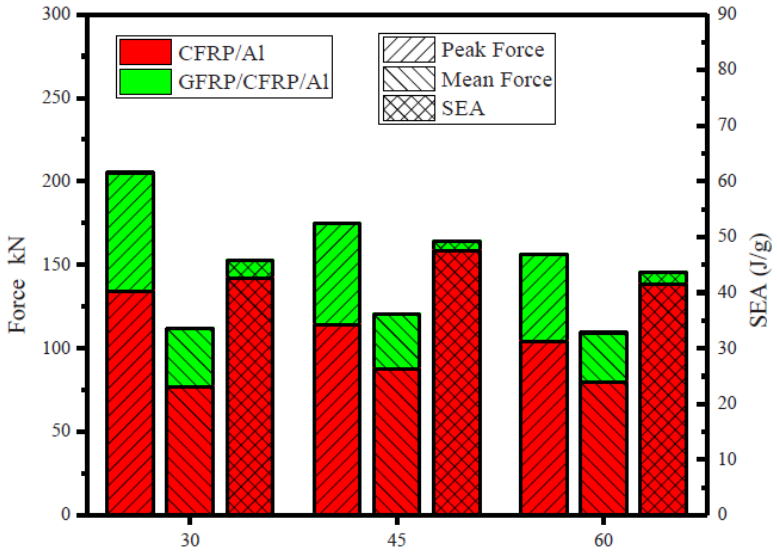


Figure 2.2. Comparison of crashworthiness characteristics of CFRP /Al and GFRP /CFRP /Al tubes [16]

Y. Ma [17] and associates determined energy absorption for five different types of carbon/aramid and carbon/carbon fiber-reinforced composite tubes by quasi-static compression tests and utilized microscope observation of the cross-section to analyze the mechanism of failure. Each specimen group had different treatment levels. They found

that the carbon/aramid CFRPs' ability to absorb energy increased after treatment and got better as treatment time increased. They also indicated that, even with the same fiber quantity and orientation, the three-layer structure of carbon/aramid FRPs demonstrated superior energy absorption performance. Therefore, they concluded that, in comparison to carbon/carbon FRP composites, carbon/aramid FRP composites with temperature treatment could achieve excellent energy absorption capabilities.

Due to applications under fire, high thermal properties are required to be tailored specifically, such as the glass fiber tubes with phenolic resin modifications. Despite the numerous advantages, the use of glass fiber-reinforced polymer tubes is limited by the major drawback of their performance under fire, in which their mechanical properties weaken rapidly. In this regard, with the consideration of phenolic resin performance with heat, a numerical analysis of the effects of the winding angle and stacking order on the mechanical properties of glass/phenolic composite tubes under tensile and radial compression loads was conducted by Abdallah and Braimah[18]. It revealed that the winding angles and stacking order had a significant impact on the tubes' behavior.

There are disposal and environmental problems because of the widespread use of composite materials. Therefore, protecting the environment and using sustainable, biodegradable, and environmentally friendly composites have become crucial for the future. Shrigandhi and Kothavale[19] studied natural fibers extracted from the leaf, like abaca, jute, and sisal, to investigate the fiber's potential for use in the filament winding process, considering the urgency of the situation. Not only the fibers, but the effect of filament winding parameters and material treatments to improve the strength of natural fibers were also addressed with results and additional research ideas.

Numerous industrial applications, including those in the fields of aerospace, automotive, marine, electrical, and fire resistant, have benefited from the adaptability, properties, and flame-retardant capabilities of phenolic resins. Various phenols, aldehydes, and catalysts can be used to create the phenolic resins with a wide range of structures and characteristics. [20]

The discovery of phenolic resin dates to the early 1800s. Ter Meer[21] developed the initial theories on the nature of the reaction after Baeyer[22] first identified phenolic-type resins as byproducts of the reaction among the phenols and aldehydes in the early 1870s. With the beginning of the modern age of composites in the 1930s and the development of advanced composites in the 1960s, the importance of phenolic resin increased, especially in aircraft applications. Non-aircraft phenolic resin applications with

natural fibers were also utilized such as brake linings, ship bearings and switchgears. The phenolic resins were widely utilized with glass fibers as reinforcement due to the fibers' different types and capabilities for specific properties. Therefore, there are many studies in the literature on glass and phenolic structures. [20] [23]

Ramalingam[24] and colleagues studied the heat shield aspect of a rocket shell with the layer bonding technique of carbon/epoxy inner and carbon/phenolic outer layers. They attempted to manufacture filament-wound carbon/epoxy and carbon/phenolic layers separately. Bond rejection occurred, mainly due to curing temperature differences. Therefore, they utilized the shell-on-shell method. Carbon/epoxy layer was manufactured with filament winding and fitted with a bulkhead. The carbon/phenolic layer was manufactured with the tape lay-up method. Layers were cured separately at their respected temperatures. Final assembly was done by bonding the layers with adhesives that cured at room temperature. The bonding requirement was tested with a lap shear strength test. With the results, successful bonding of two layers was observed.

Dong[25] and colleagues studied carbon fiber-reinforced phenolic resin composites with situ-curing 3D printing technology. They investigated the pre-curing temperature and deviation distance of the 3D printing process to produce continuous carbon-fiber phenolic resin structures. Therefore, improvements in flexural properties were also evaluated. Hu[26] and colleagues studied the curing mechanism and chemical structure of phenolic resin with different synthesis reactions in the range of 90–230 $^{o}$C. The reactions were observed and divided into four stages with their detailed formations and curing temperature ranges. They aimed to offer an innovative approach for evaluating phenolic resin's curing process.

As the few examples from the literature demonstrate, not only parameter or material components investigated, but chemical, thermal, and mechanical treatments and modifications also studied in various cases.

# CHAPTER 3

# EXPERIMENTAL STUDY

In this study, to evaluate and analyze the different stacked resin effects on the mechanical and thermal properties of carbon composite tubes, two different configurations were manufactured by using carbon fiber filament and two different resin types.

## 3.1. Materials

The required materials for this study were chosen to be suitable for the filament winding process. The utilized filament material was 12k A-49 labeled 800 tex carbon fiber filament yarn, which was obtained from DowAksa, a carbon fiber manufacturer.

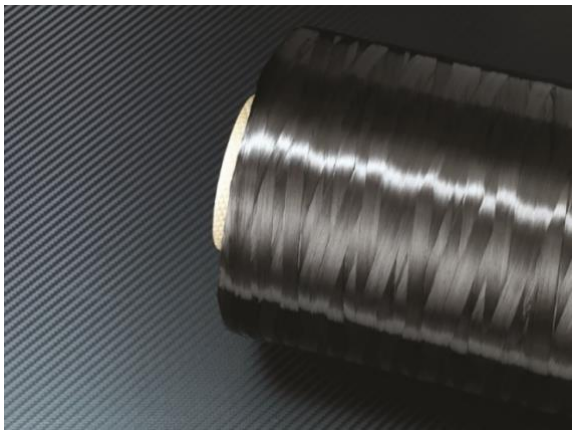

Figure 3.1. Representation of carbon fiber filament yarn provided by DowAksa

Phenolic resins are the best suited for high-temperature applications where parts must conform to regulations for toxicity, combustion, smoke emission, and fire safety. They exhibit good heat and chemical resistance, electrical non-conductivity, and flame-retardant properties. Phenolic materials have a low density, excellent thermal insulation, exceptional durability, and are simple to shape into complex forms. Therefore, as the matrix materials, epoxy resin and phenolic resin were chosen.

The epoxy resin is the three-component mixture from Huntsman™. The first component is Araldite™ MY-740 epoxy resin, the second is Araldur™ MY-918 curing

agent (hardener) and the last one is DY-070 accelerator. The weight ratio for the chemical mixture between epoxy resin and curing agent is 90%. After homogeneity was achieved by mixing the resin and hardener, the accelerator was added at a ratio of 0.5-2.5% of the weight of the resin. To eliminate the production difference, the accelerator was used at 2% in all the composite pipe productions.

The derivatives of phenolic resin, which used in industry, are very dangerous and carcinogenic for human health in general. Thus, the phenolin resin, which is the safe form of this substance without dangerous ingredients, was utilized in this study. The phenolin resin is a two-component mixture that was provided by Epakem Kimya. The first component is Fenolinn FX-300 phenolin mechanic resin, and the second is FXH-300 curing agent (hardener). The weight ratio of the chemical mixture between phenolin resin and hardener is 5.2%. Because of the short curing cycle of this mixture, an accelerator is not required.

## 3.2. Filament Winding Machine and Equipment

The filament winding process requires automation or computer-aided production to achieve continuity in the fiber winding process without any disruption or external factors. Because of the automatic manufacturing process, CADWIND$^{TM}$ or similar software is required to create complex structures with desired properties. Thus, in this study, a filament winding machine with a 4-axis movement capacity and the tension machine, both by Fibermak Composites, were utilized to produce filament-wound carbon composite tubes. For resin application, metal resin bath equipment is attached, which is part of the machine.

The filament winding machine, resin bath, and attached aluminum mandrel with impregnated fibers were prepared for the manufacturing of the tubes, as shown below in Figure 3.2. As the second piece of support equipment besides the tension machine, the exclusive programmable curing oven by Fibermak Composites was used for the curing cycle of the composite parts, as shown below in Figure 3.3.


Figure 3.2. Filament winding machine and the setup for composite tube

Figure 3.3. Programmable curing oven

## 3.3. Manufacturing Processes

To investigate the effects of resin on mechanical and thermal properties, carbon fiber filament-wound tubes with two different layer configurations were manufactured. The carbon fiber plates with only epoxy resin or phenolin resin were also manufactured to obtain each layer's properties.

### 3.3.1. Manufacturing of Composite Tubes

The carbon fiber filament-wound composite tubes were manufactured with the filament winding method. Pre-determined manufacturing properties of these tubes, such

as winding angle, length of composite tube, number of layers, winding pattern, coverage ratio, speed of winding, and tension level, require precise manufacturing with an automated process. Therefore, these properties were first programmed and analyzed in simulation by utilizing CADWIND™ V9 filament winding software. The winding speed and tension are adjustable within filament winding and tension machines before or during the manufacturing process.

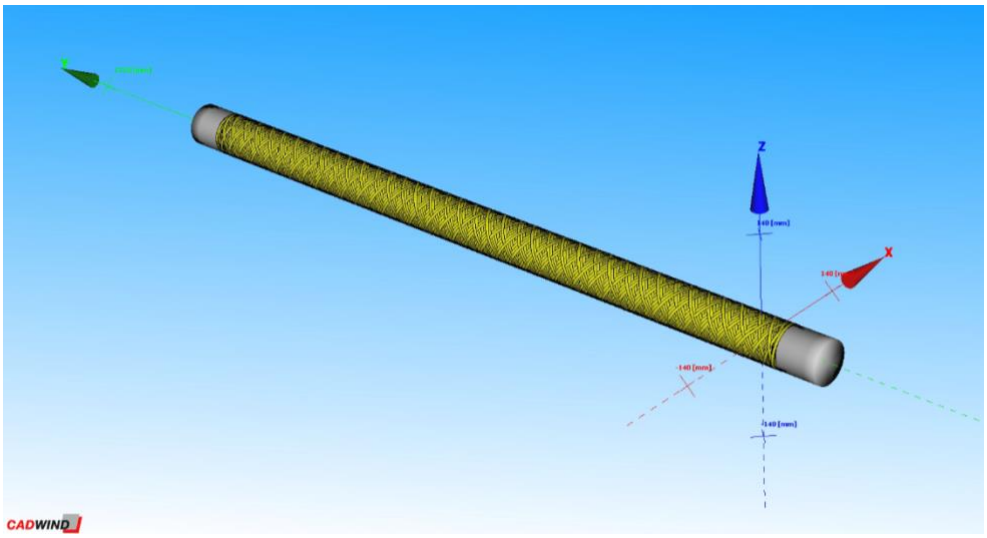


Figure 3.4. Simulation of winding program with CADWIND$^{TM}$ V9

After the preparation of the machine and the cylindrical aluminum mandrel, the next step was to prepare the resin and the resin bath equipment. The epoxy resin was prepared according to weight ratio, with its three components, resin, hardener, and accelerator, at 100:90:2, respectively. To prevent waste of resin material, 250 gr of epoxy resin, 225 gr of hardener, and 5 gr of accelerator were used, according to the previous manufacturing processes and the analysis of the composite tubes. After homogeneity was achieved by mixing inside a beaker, the mixture was left for the dispersion of the air bubbles to prevent any contamination or flaw in the process. After the bubbles were gone, the mixture was poured into the resin bath.

To keep the pressure in the filament constant, the carbon fiber yarn was attached to the tension machine. The machine was adjusted to a constant 6 N force. The carbon fibers were impregnated by passing through the resin bath and prepared for winding.

At the beginning of the winding process, the impregnated carbon fibers were automatically adjusted by the machine according to the winding program at the 55$^{o}$

winding angle. The length of the composite tube and such limitations were also considered in the program.

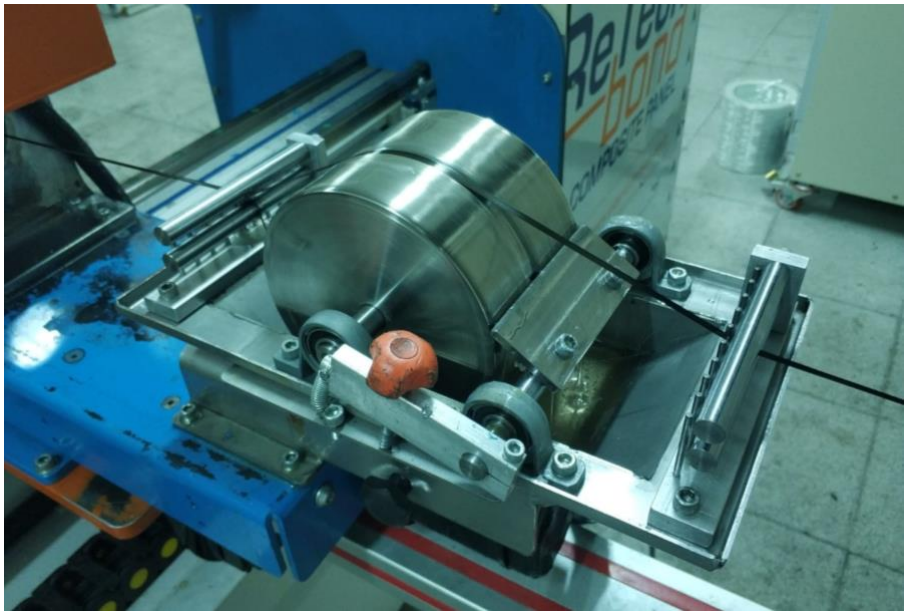

Figure 3.5. Impregnation of carbon fibers within resin bath

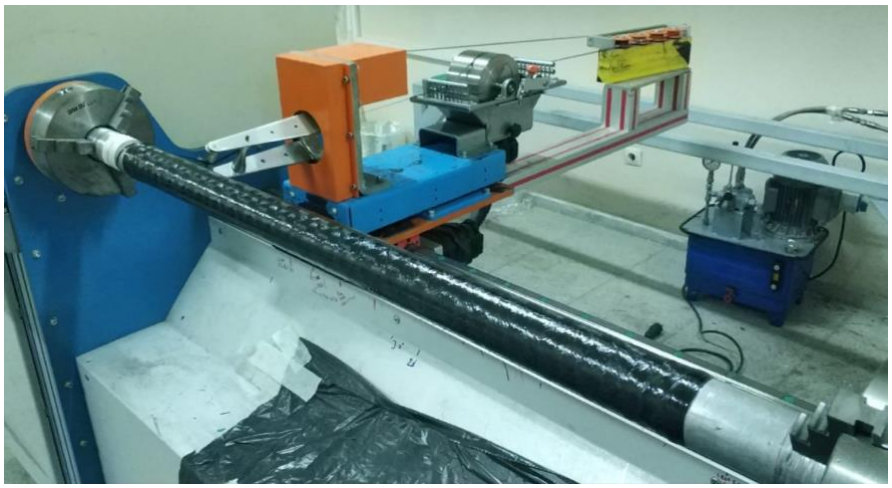

Figure 3.6. The completed filament-wound carbon fiber tube

After the filament winding process was completed, the composite tube was cured in the curing oven. The oven was set at 80 $^{o}$C for 2 hours and 120 $^{o}$C for 4 hours, with constant rotation to prevent aggregation of epoxy. When the curing was done, the composite tube was left to cool slowly to room temperature in the oven. After the cooling was done, the tube separated from the aluminum mandrel with the exclusive hydraulic

separator without any damage. Excessive and irregular ends of composite tubes were cut with a diamond saw.

First, the 5-layer carbon fiber epoxy resin filament-wound tubes were produced. After the 5-layer carbon epoxy resin tubes were completed, the same procedure was applied for the second group as 4-layer carbon epoxy resin with 1-layer phenolin resin. For the second group, the first four inner layers of composite tube were epoxy resin, and the fifth layer, which was the outer layer of composite tube, was phenolin resin. Two samples produced for each group.

It should be considered that, due to the fast-curing cycle of phenolin resin, the density difference compared to epoxy resin, and the limitations of the manufacturing equipment, composite tubes with full 5-layer phenolin resin could not be manufactured. Despite the production efforts for the different layer setups with phenolin, the outcomes were unfortunately not reliable due to inhomogeneity and impregnation failure. Therefore, the effects of the addition of only one layer of phenolin resin were investigated in this study.

### 3.3.2. Manufacturing of Composite Plates

As mentioned above, carbon fiber plates were also manufactured to obtain each resin layer's properties with filament winding. The properties obtained for future investigations of finite element analysis. The same procedure of composite tube manufacture was also followed for composite plates. The differences were the square steel plate, which connected the machine by a short mandrel, and the suitable program with CADWIND$^{TM}$ for the plate winding.

The plates were manufactured in four layers to obtain a suitable thickness for test procedures. After the manufacturing, the curing oven was set with the same program for composite tubes, which was 80 $^{o}$C for 2 hours and 120 $^{o}$C for 4 hours.

Since the hydraulic separator was not suitable for square plates, teflon film was coated around the plates before the start of the winding process. Teflon film helps the separation of carbon plates by preventing the impregnated fibers from sticking to the plate surface. The excessive sides of the panel were cut with a handsaw without any damage to the main section of the plate.

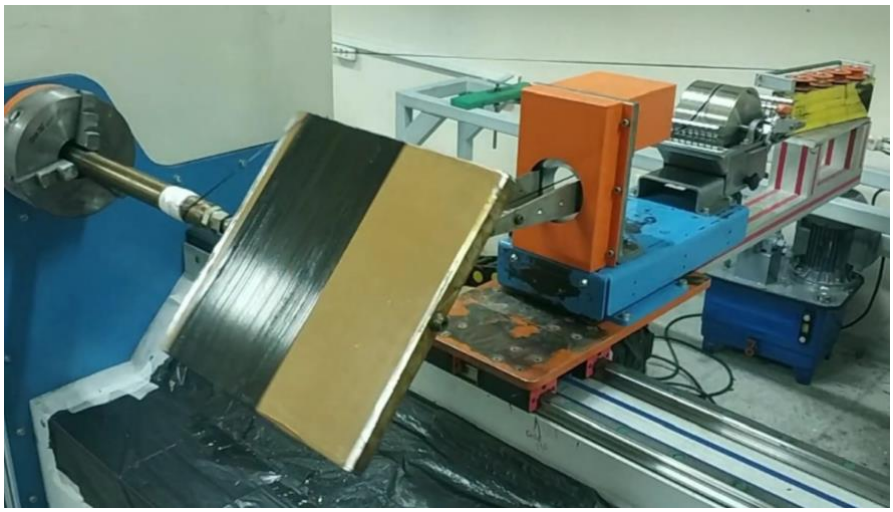

Figure 3.7. Filament-wound carbon fiber plate manufacturing

## 3.4. Applied Tests to Composite Tubes

In this study, the mechanical and thermal properties of filament-wound composite tubes were investigated according to their standards. The test setups were prepared and tested to be suitable for sample dimensions to prevent any issues related to equipment.

### 3.4.1. Mechanical Testing of Composite Tubes

To obtain the mechanical properties of composite tubes, three mechanical tests were applied: The apparent hoop tensile test, the radial compression test, the three-point bending test. Two composite tubes were manufactured for each group. To prevent any concern about the continuity of each tube's mechanical properties, the samples were prepared from different areas of the tubes.

#### 3.4.1.1. Apparent Hoop Tensile Test

The apparent hoop tensile test with the split disk method can be applied to cylindrical structures to obtain apparent hoop tensile strength. In this study, the apparent hoop tensile test was applied according to ASTM D2290 Procedure A (ASTM D2290-00 2003). Shimadzu™ AG-IC Series universal test machine with a load cell of 100 kN was utilized for apparent hoop tensile test at room temperature by using specialized split disk test apparatus as shown below in Figure 3.8.

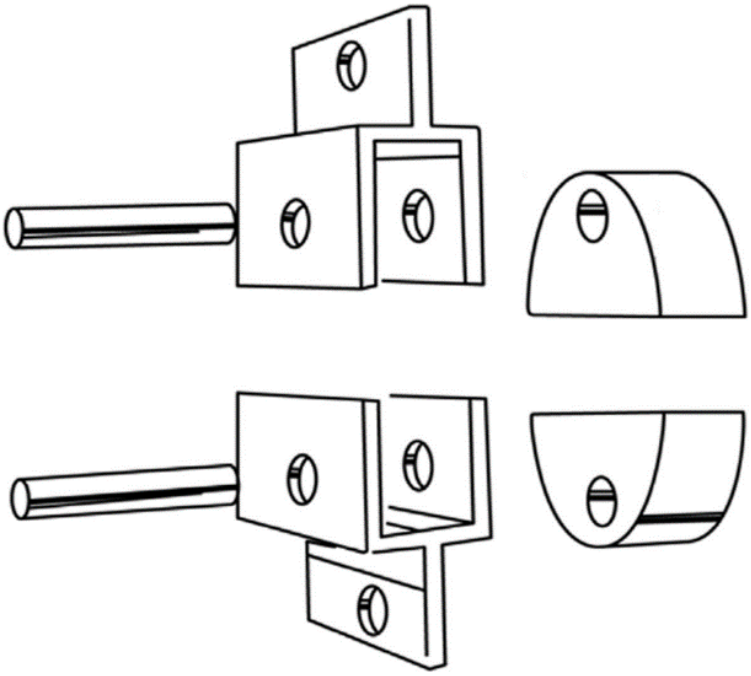

Figure 3.8. Schematic representation of apparent hoop tensile test setup [ASTM D2290-2003]

For the hoop tensile test, at least three samples were prepared from each group of composite tubes. The reserved parts of composite tubes for the hoop tensile test were drilled with a CNC machine according to ASTM standard.

Due to the thin layers of the composite tube, a precise drilling process is required to prevent delamination between layers. Therefore, three different diameters were used in the drilling process with precise speed: 4 mm, 7 mm, and 9 mm. After the process, the drilled parts were sectioned as ring samples according to ASTM standard with a diamond saw.

The tests were proceeded until the failure behavior or break point of the samples were observed. The test data were recorded and taken from the test machine as force (N) and displacement (mm).

The Calculation of the apparent hoop tensile strength of the ring samples was obtained according to Equation 3.1:

$$\sigma_a = \frac{P_b}{2A_{min}} \tag{3.1}$$

where $P_b$ is the maximum or breaking load in Newton, $A_{min}$ is the minimum cross-sectional area in square millimeters, and $\sigma_a$ represents the ultimate hoop tensile strength.

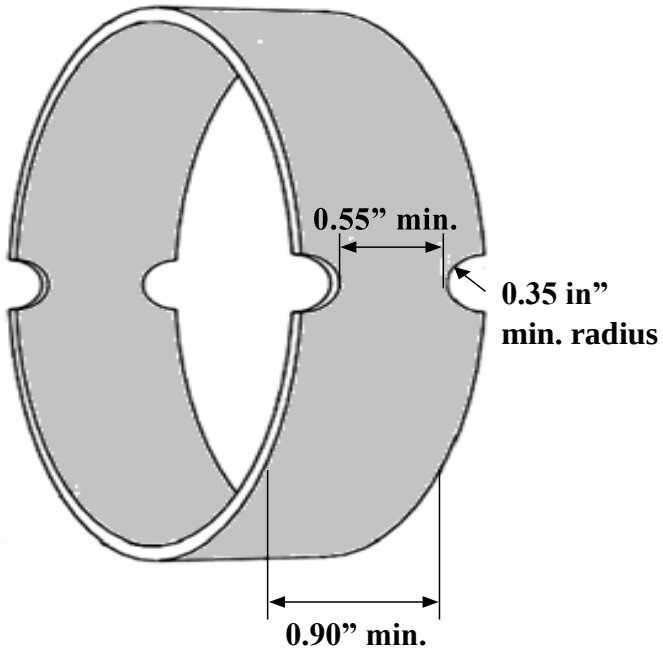


Figure 3.9. Dimensions of ring test samples [ASTM D2290-2003]

The test samples were tested with a constant crosshead speed, which was set to 5 mm/min. Prepared test samples according to the standard ASTM D2290 are shown below in Figure 3.10. with the following representation codes for groups: (5CE) was a 5-layer epoxy resin, and (4CE 1CP) was 4-layers of epoxy resin and 1-layer of phenolin resin.

The ring specimens were placed onto the split disk test apparatus, which was assembled on the tensile test fixture as shown in Figure 3.11. The alignment of the split disks and apparatus was also considered to eliminate any concern. Also, the fitment of the samples to the apparatus were tested to check if any issue may occur.

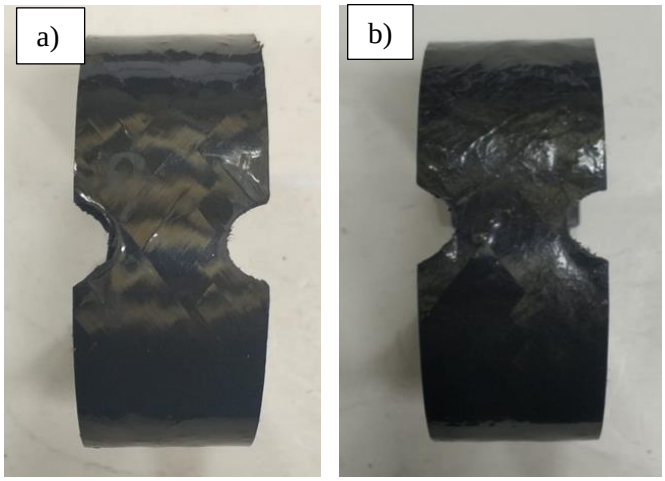


Figure 3.10. Sectioned ring specimens before apparent hoop tensile test, a) 5CE, b) 4CE 1P

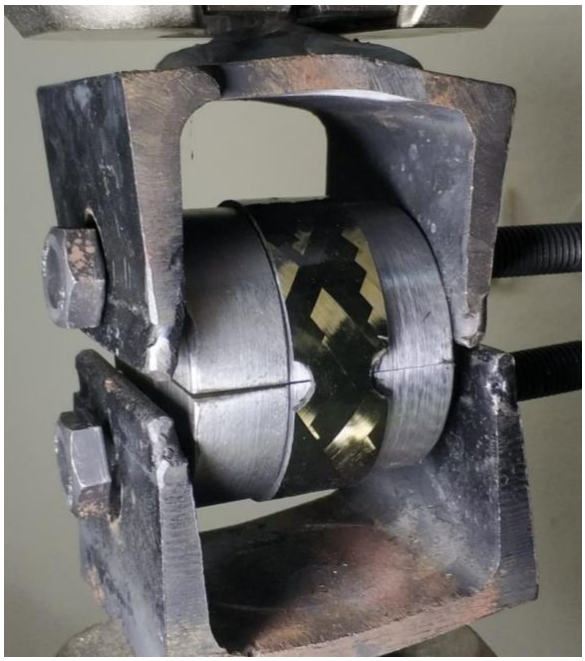

Figure 3.11. Split disk test setup with sectioned ring sample

### 3.4.1.2. Radial Compression Test

The radial compression test can be applied to cylindrical structures to determine the stiffness of composite materials. In this study, the radial compression test was applied according to ASTM D2412 (ASTM D2412-02 2008). Shimadzu™ AG-IC Series universal test machine (100 kN) with compression apparatus utilized for radial compression test. A representation of the radial compression test setup is shown below in Figure 3.13.

At least three samples were prepared from different areas of each group of composite tubes according to the ASTM D2412 standard. All the test samples were cut with a diamond saw to 80 mm in length. The test data was recorded and taken from the test machine as force (N) and displacement (mm). The test was stopped at the failure or significant load drop of the samples. The calculation of the stiffness (PS) of the composite tube samples was obtained according to Equation 3.2:

$$PS = \frac{F}{\Delta y} \tag{3.2}$$

where $F$ is the maximum or crack load in Newton, and $\Delta y$ is the deflection in mm of the inner diameter of the samples. The Calculation of the percent of deflection (PD) of the composite tube samples was obtained according to Equation 3.3:

$$PD = \frac{\Delta y}{d} \tag{3.3}$$

*PD* is the percentage of deflection, *d* is the internal diameter of the sample in millimeters, and *Δy* is the total deflection where the failure occurred.

Prepared test samples are shown in Figure 3.12 with the following representation codes for groups: (5CE) was 5-layer epoxy resin, and (4CE 1CP) was 4-layers of epoxy resin and 1-layer of phenolin resin. Composite test specimens were placed between the upper and lower apparatus, which are the 100 mm diameter steel circular fixtures of the test machine.

A compression force was applied in the radial direction and through the composite tube until failure or a significant load drop occurred. The crosshead speed of the universal test machine was fixed at 12.5 mm/min, according to the standard.

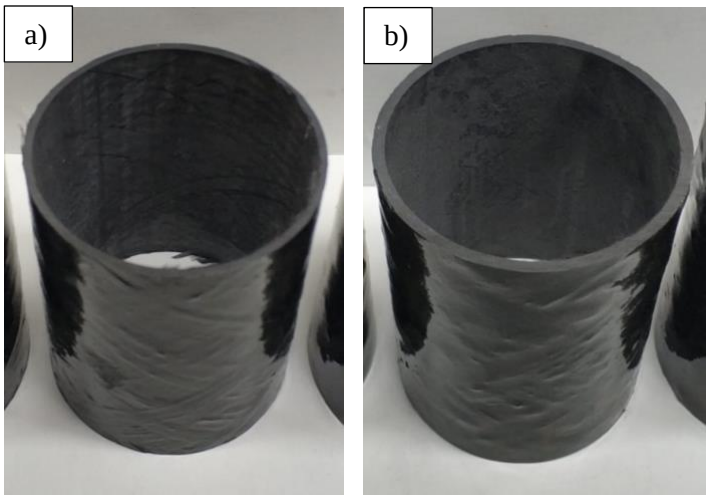


Figure 3.12. Sectioned test samples before radial compression test, a) 5CE, b) 4CE 1P

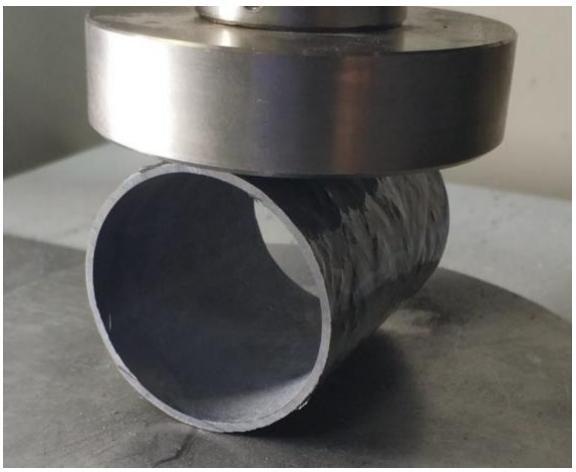

Figure 3.13. Test setup of radial compression test

### 3.4.1.3. Three-Point Bending Test

The three-point bending test can be applied to various parts such as sheets, plates, pipes, rectangular bars, or molded shapes to obtain the flexural properties of the material. In this study, the three-point bending test was applied according to ASTM D790 (ASTM D790-03). Shimadzu™ AG-IC Series universal test machine (100 kN) with three-point bending apparatus utilized for bending test. The test setup is shown in Figure 3.15.

For the bending test, at least three samples were prepared from each group of composite tubes. The samples were cut to 300 mm in length with a diamond saw.

The test data was recorded and taken from the test machine as force (N) and displacement (mm). The test was stopped at the failure or significant load drop of the samples. The flexural strength of the composite tube samples was calculated according to Equation 3.4:

$$\sigma_f = \frac{M_y}{I_x} \tag{3.4}$$

$$I_x = \frac{(D_o{}^4 - D_i{}^4)\pi}{64} \tag{3.5}$$

where $M$ (Nm) is the bending moment of the tube, $y$ (mm) is the vertical distance away from the neutral axis, $I_x$ (mm$^4$) is the moment of inertia, and $D_o$ and $D_i$ are the outer and inner diameters of the tube, respectively.

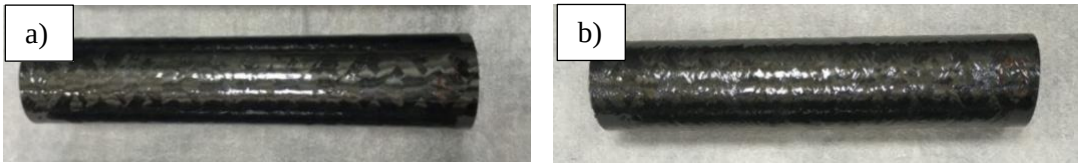


Figure 3.14. Reserved samples before 3-point bending test, a) 5CE, b) 4CE 1P

Prepared test samples are shown above in Figure 3.14 with the following representation codes for groups: (5CE) was a 5-layer epoxy resin, and (4CE 1CP) was 4-layers of epoxy resin and 1-layer of phenolin resin.

Composite tube samples were placed in the middle of the lower supports, which were set for a 240 mm span length. The setup was positioned so that the upper support attached to the crosshead was also in the middle.

The bending force applied to the composite tube until failure or a significant load drop occurred. The crosshead speed of the universal test machine was fixed at 5 mm/min according to the standard.

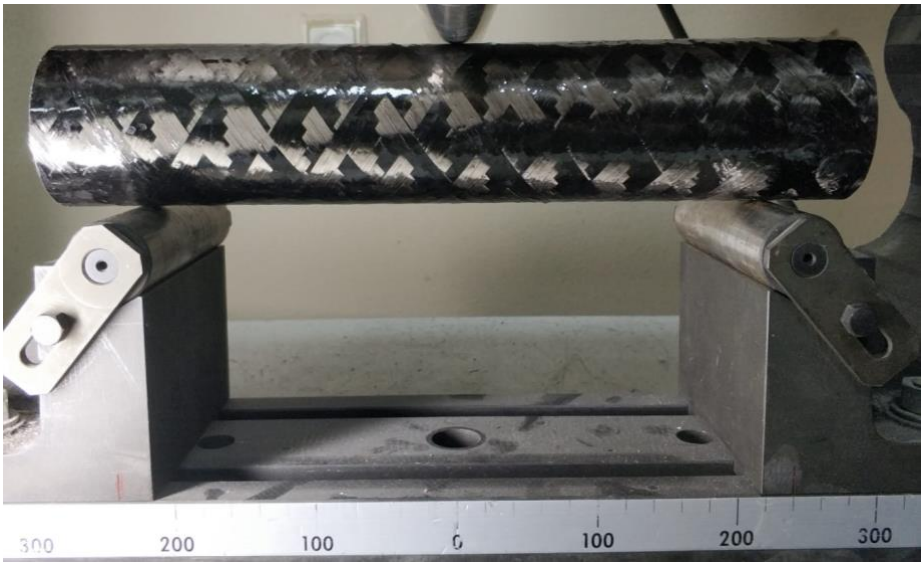


Figure 3.15. Test setup of 3-point bending test

### 3.4.2. Thermal Testing of Composite Tubes

In this study, the objective was thermal enhancement of the composite filament wound tubes. For this purpose, thermal experiments were conducted for phenolin resin and epoxy resin comparison. Therefore, thermal properties were investigated. To obtain the thermal properties between two different resin groups of composite tubes, three thermal tests were applied:

The Thermogravimetric Analysis (TGA) test, the Differential Scanning Calorimeter (DCA) test, the thermal conductivity test, and the flammability test.

To prevent any concern about the continuity of each tube's thermal properties, the samples were prepared from different areas of the tubes. Thus, the homogeneity of the tubes could also be tested.

#### 3.4.2.1. Thermogravimetric Analysis (TGA) Tests

Thermogravimetric analysis (TGA) is a thermal test, which the weight of a sample is measured over time as the temperature changes in a controlled atmosphere. Both

chemical and physical events, including heat decomposition and solid-gas reactions, can be observed by this measurement, including phase transitions, absorption, and desorption.

The test procedure and equipment were provided by the Center for Materials Research (CMR) within the Izmir Institute of Technology (IZTEC). In this study, the PerkinElmer Diamond Thermogravimetric/Differential Thermal Analysis (TG/DTA) system test equipment was utilized.

Figure 3.16. PerkinElmer Diamond (TG/DTA) system

For this test, samples were prepared on a milligram scale from composite tubes. To investigate thermal effects, 700 $^{o}$C with a 5 $^{o}$C/min step and a 25 $^{o}$C start point of temperature setup were determined. The tests were conducted in a nitrogen-gas environment.

The results were calculated and corrected statistically and graphically. Thus, additional results could be obtained with detailed investigations. For further study, derivative of the graphical results was also obtained.

### 3.4.2.2. Differential Scanning Calorimeter (DSC) Test

The differential scanning calorimeter (DSC) is a thermal test to investigate how the heat capacity of materials is changed by temperature. In this procedure, heat capacity is recorded with material mass, and heat flow changes with temperature. The materials'

heat capacity and heat flow properties are also recorded during the heating or cooling process. Thus, thermal properties can be observed, such as melting point, glass transition, phase transition, and curing.

The test procedure and equipment were provided by the Geothermal Energy Research and Application Center (GEOCEN) within the Izmir Institute of Technology (IZTEC). In this study, the TA Instruments Q10 DSC test equipment was utilized.

Figure 3.17. DSC test equipment (TA Instruments Q10)

For this test, carbon fiber tube samples were prepared on a milligram scale from composite tubes. To investigate thermal effects, 500 $^{o}$C with a 5 $^{o}$C/min increase and a 25 $^{o}$C start point of the temperature setup were determined.

The results were calculated and corrected statistically and graphically. Thus, additional results could be obtained with detailed investigations.

### 3.4.2.3. Thermal Conductivity Test

A thermal conductivity test can be applied to various materials to determine their ability to transmit heat, and it is measured in watts per meter of kelvin (W/mK). It is used to measure the heat transfer coefficient of materials with low thermal conductivity.

The test procedure and equipment were provided by the Geothermal Energy and Research Center (GEOCEN) within the Izmir Institute of Technology (IZTEC). In this study, KEM QTM 500 thermal conductivity meter test equipment was utilized.


Figure 3.18. Thermal conductivity meter test equipment (QTM 500)

Three samples were prepared from different areas of composite tubes. The samples were cut to the required dimensions of the test equipment.

### 3.4.2.4. Flammability Test

The flammability test investigates whether the substance tends to either extinguish or spread the flame once the specimen has been ignited. These properties were studied with the UL-94 (UL-94 2013) standard, which was conducted to quantify and rank the flame retardancy of the composites. Due to the toxic fumes of ignited materials and potential fire hazards, the TESTEX UL-94 Flammability Cabin was utilized for this test. The UL-94 standard describes five procedures for controlling the burning behavior of materials. For this study, the Horizontal Burning (HB) procedure was considered.

For this test, at least five samples were prepared from each group, as shown below in Figure 3.20, with the following group representation codes: (5CE) was a 5-layer epoxy resin, and (4CE 1CP) was 4-layers of epoxy resin and 1-layer of phenolin resin.

To observe the outer layer effect on samples, the test procedure was modified to use half-tube samples for this study. Therefore, the samples were cut to 80 mm in length as half tubes.

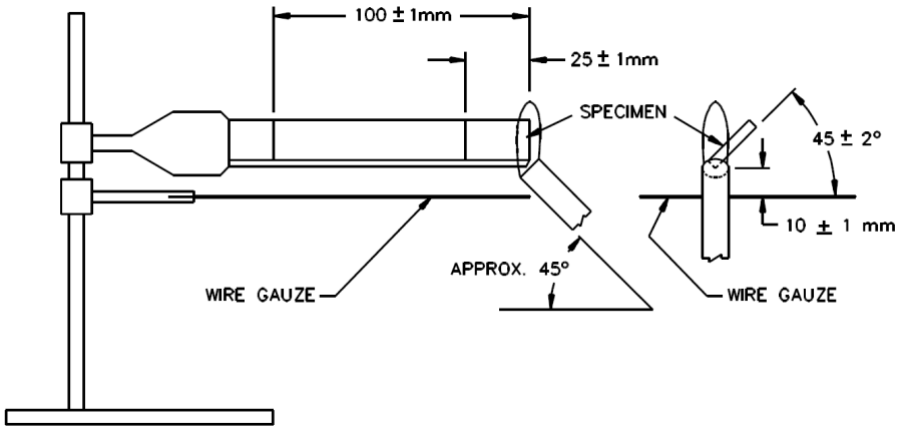


Figure 3.19. Horizontal test setup according to UL-94 HB [UL-94 2013]

After the sample was attached to the clamps inside the cabin with the outer layer facing the flame, the flame nozzle was positioned in the middle of the sample at 90$^{o}$ degree angle to the surface with a 10 mm distance from the lowest edge of the sample.

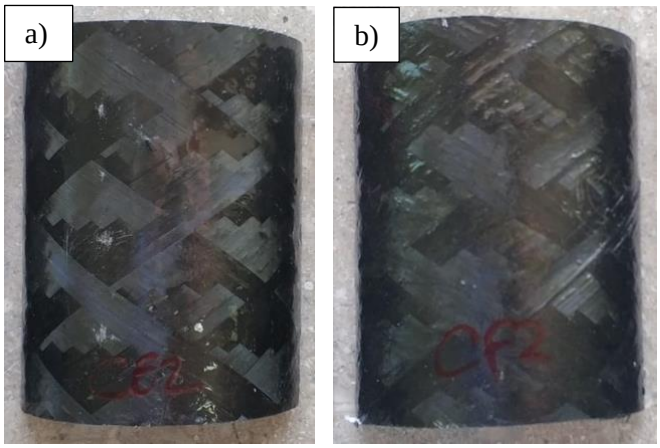


Figure 3.20. Prepared flammability test samples, a) 5CE, b) 4CE 1P

The sample ignited for three scenarios: flame contact for 30 seconds, 60 seconds, and 600 seconds. Then the flame nozzle moved away from the sample. The time in seconds was recorded until the flame extinguished completely. After the extinguishment, the flash point time, extinguishment time, and damage to the burned material were observed and recorded.

## 3.5. Calculation of Fiber Mass Fraction

The fiber mass fraction of composite tubes was measured using the matrix digestion (acid digestion) test. The test was conducted according to ASTM D3171 (ASTM D3171- 2015) standard. Since carbon fiber was not suitable for burn-off test, acid digestion procedures were considered. Procedure B was chosen to proceed because of its efficiency compared to Procedure A with nitric acid. The procedure consists of two components: sulfuric acid ($H_2SO_4$) and hydrogen peroxide ($H_2O_2$).

In this test, two composite specimens from each group were prepared before the digestion test. At least three test specimens from each composite tube were prepared, each weighing approximately 2 grams. Before the start of a digestion test or chemical process, precautions were taken with acid gloves and a full-face gas mask.


Figure 3.21. Acid digestion process of two samples before hydrogen peroxide addition

According to the ASTM standard, 100 ml of sulfuric acid should be put into a glass beaker with at least 250 ml of volume to prevent overflow. A beaker was placed on a hotplate with the temperature set to 100 °C. When the solution had a near black color or no visibility inside the mixture and the sample dispersed as fibers without any solid part, approximately 30 ml of hydrogen peroxide were added in the form of a drop with a syringe. Because of the acidic fumes from the chemical reaction of hydrogen peroxide drops, all the processing was done under the fume hood.

Hydrogen peroxide was applied to the mixture until the solution was colorless and floating fibers appeared above the solution. The acidic solution was poured into the contamination bottle with a fine sieve and left to cool to room temperature. Fibers were

washed with distilled water and dried in an oven at 100 °C for 1 hour. After drying, each specimen was weighed, and the fraction was calculated with Equation 3.7:

$$W_r = (M_f / M_i)\, x\, 100 \quad (3.7)$$

where $W_r$ is the weight percentage of fiber, $M_i$ is the final mass, and $M_f$ is the initial mass of the sample.

## 3.6. Scanning Electron Microscopy (SEM)

Scanning Electron Microscopy (SEM) is a microscope technique that forms images with the use of electrons instead of light. SEM is used to obtain images of the microstructural structure of materials. The images can be taken for the study, such as to determine the quality of manufacture or investigate the failure mechanism and effects in the microstructure. The test procedure and equipment were provided by the Center for Materials Research (CMR) within the Izmir Institute of Technology (IZTEC). In this study, FEI QUANTA 250 FEG test equipment was utilized. The samples for this test were cut from each tube and placed onto a cap to fix the vertical angle of the samples to the equipment lens.

Figure 3.22. SEM test equipment (FEI QUANTA 250 FEG)

# CHAPTER 4

# RESULTS AND DISCUSSION

In this chapter, mechanical and thermal results were investigated and detailed, both graphical and statistical. Before that, microstructural homogeneity and validity were also investigated.

## 4.1. Microstructural Properties of Filament Wound Composite Tubes

Apart from mechanical and thermal properties, microstructural characterization was done by acid digestion, Scanning Electron Microscopy (SEM) and optical microscope.

### 4.1.1. Fiber Mass Fraction Test Results

To investigate the fiber content, acid digestion was performed according to the ASTM D3171 standard, which is detailed in Section 3.5.

Table 4.1. Fiber mass fractions of filament-wound composite tubes

| Sample Name | Weight Percentage of Fiber (%) |
|---|---|
| 4CE 1CP | 68.06 |
| 4CE 1CP | 69.51 |
| 5CE | 73.11 |
| 5CE | 72.69 |

Results after the drying process are listed in Table 4.1. The average fiber content was calculated as approximately 70.84 wt% with a 2.46 standard deviation. With a low deviation between groups and suitable results according to research, studies were continued.

### 4.1.2. Scanning Electron Microscopy Images

The SEM images with different magnifications were taken from various sections of the cross-sectional samples. The results were provided by the Center for Materials Research (CMR) within the Izmir Institute of Technology (IZTEC). The following images in Figure 4.1 and Figure 4.2 were selected from the same region of samples to check for differences. The images demonstrate that the cross-sectional microstructures of composite tubes were similar.

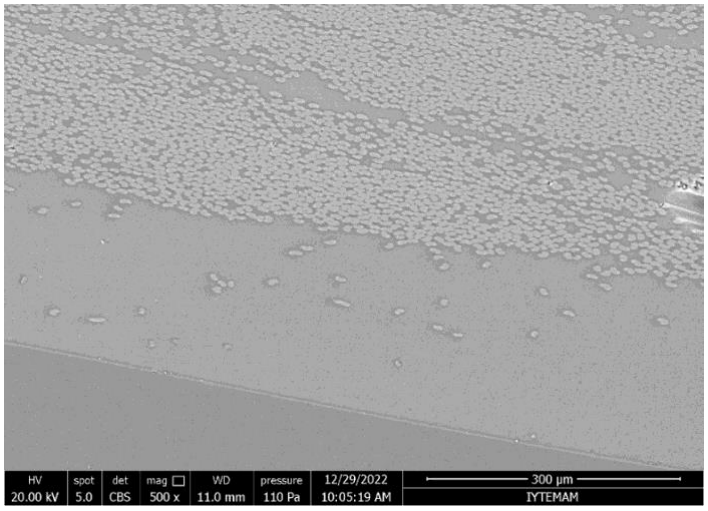


Figure 4.1. Cross-sectional SEM image of 5-layer carbon epoxy sample

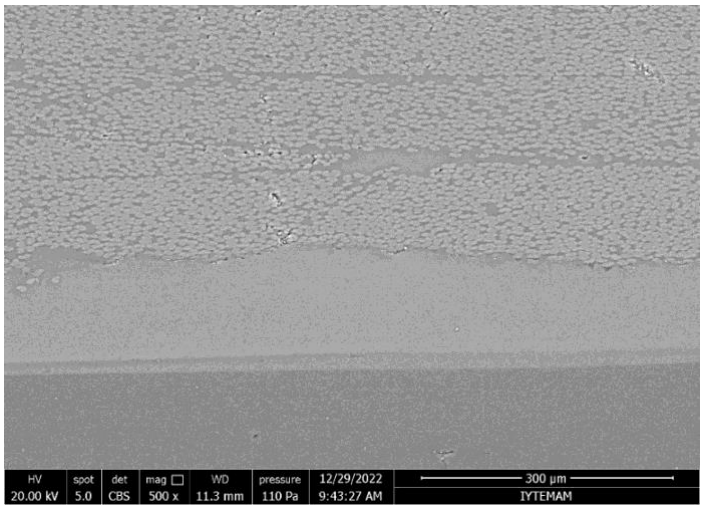


Figure 4.2. Cross-sectional SEM image of 4-layer carbon epoxy with 1-layer phenolin resin sample

## 4.2. Mechanical Properties of Filament Wound Composite Tubes

Since satisfying microstructural results and desired configurations were obtained, the mechanical tests were prepared and applied. The results are detailed for each test, both numerically and graphically.

### 4.2.1. Apparent Hoop Tensile Test Results

The apparent hoop tensile test was applied with the split disk method. Hoop tensile strength was calculated for each group with Equation 3.1 according to ASTM D2290. For the calculation, recorded load and displacement data from the test machine were used. The minimum cross-sectional area and strength results are given for each group in Tables 4.2 and 4.3.

Table 4.2. Apparent hoop tensile test results of 5-layer carbon epoxy resin samples

| Sample Name | Hoop Tensile Strength (Mpa) | $A_{min}$ ($mm^2$) |
|---|---|---|
| 5CE_1 | 443.51 | 23.19 |
| 5CE_2 | 451.11 | 23.52 |
| 5CE_3 | 532.14 | 22.10 |
| **Average** | **475.59** | **22.94** |
| **St. Dev. (±)** | **49.12** | **0.75** |

Table 4.3. Apparent hoop tensile test results of 4-layer carbon epoxy with 1-layer phenolin resin samples

| Sample Name | Hoop Tensile Strength (Mpa) | $A_{min}$ ($mm^2$) |
|---|---|---|
| 4CE_1CP_1 | 499.07 | 24.92 |
| 4CE_1CP_2 | 484.64 | 22.79 |
| 4CE_1CP_3 | 449.79 | 22.27 |
| **Average** | **477.83** | **23.32** |
| **St. Dev. (±)** | **25.33** | **1.41** |

The force-displacement graphical results of apparent hoop tensile test with the failure points are shown in Figure 4.3 and Figure 4.4.

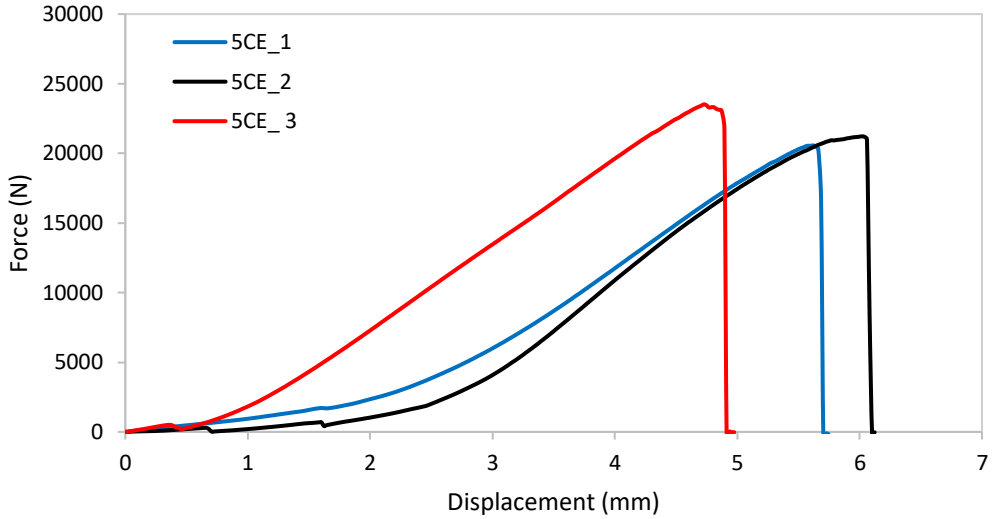


Figure 4.3. Force-Displacement graph of 5-layer carbon epoxy resin samples

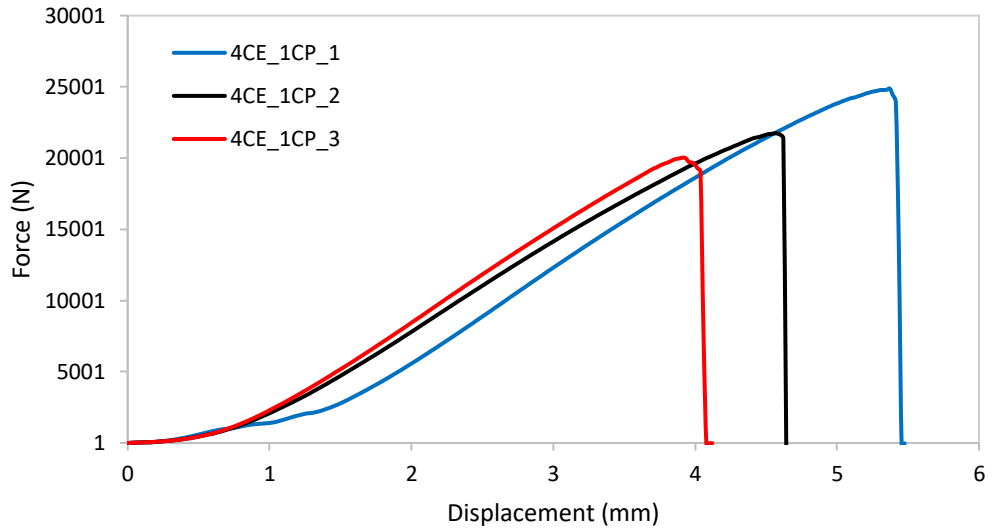


Figure 4.4. Force-Displacement graph of 4-layer carbon epoxy with 1-layer phenolin resin samples

To investigate the effect of phenolin resin in tensile strength, two groups were calculated according to ASTM standard, as shown in Table 4.4.

Table 4.4. Comparison of tensile test results (average ± standard deviation)

| Sample Name | Hoop Tensile Strength (Mpa) |
|---|---|
| 5CE | 475.59 ± 49.12 |
| 4CE_1CP | 477.83 ± 25.13 |
| **Difference (%)** | **0.47** |

The average apparent hoop tensile strength values of composite tubes were calculated as ±475.59 MPa for the 5-layer carbon epoxy group and ±477.83 MPa for the 4-layer carbon epoxy with the 1-layer carbon phenolin resin group.

Results in this study demonstrate that a significant effect was not observed for hoop tensile strength at phenolin resin addition compared to the fully carbon fiber epoxy resin group. The average strength difference was only 0.47%. Failure modes of ring samples after the hoop tensile test were observed as in Figure 4.5.

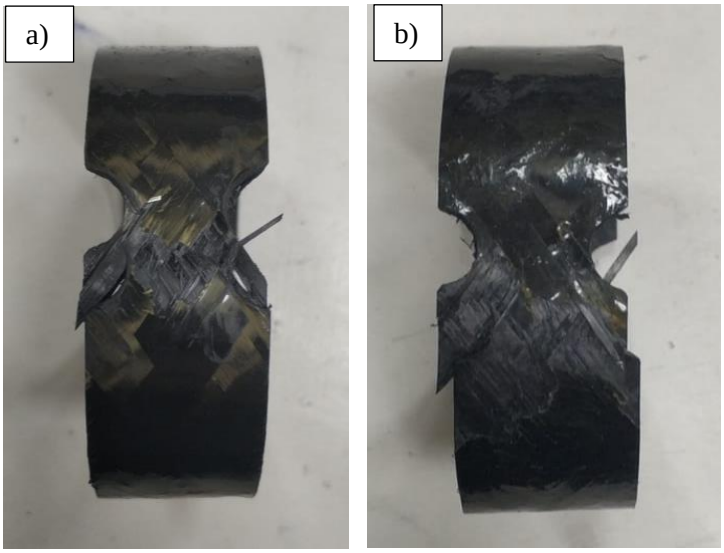


Figure 4.5. Sectioned ring samples after apparent hoop tensile test, a) 5CE, b) 4CE 1P

After the test, the failure behavior of the samples was investigated. The crack was observed in the reduced area of the sectioned rings, as expected. The crack of fibers occurred along the line of 55$^{o}$ orientation angles of composite tubes.

### 4.2.2. Radial Compression Test Results

The radial compression test was applied to the sectioned tube samples to determine stiffness. Pipe stiffness was calculated for each group with Equation 3.2 according to ASTM D2412. For the calculation, recorded load and displacement data from the test machine were used. Deflection and stiffness results are given for each group in Tables 4.5 and 4.6.

Table 4.5. Radial compression test results of 5-layer carbon epoxy resin samples

| Sample Name | Pipe Stiffness (N/mm) | Percentage of Deflection (%) |
|---|---|---|
| 5CE_1 | 423.43 | 8.05 |
| 5CE_2 | 508.81 | 6.30 |
| 5CE_3 | 455.14 | 9.15 |
| **Average** | **462.46** | **7.84** |
| **St. Dev. (±)** | **43.16** | **1.44** |

Table 4.6. Radial compression test results of 4-layer carbon epoxy with 1-layer phenolin resin samples

| Sample Name | Pipe Stiffness (N/mm) | Percentage of Deflection (%) |
|---|---|---|
| 4CE_1CP_1 | 426.07 | 7.39 |
| 4CE_1CP_2 | 469.05 | 7.95 |
| 4CE_1CP_3 | 521.06 | 7.34 |
| **Average** | **472.06** | **7.56** |
| **St. Dev. (±)** | **47.57** | **0.34** |

The force-displacement graphical results of radial compression test with the failure points are shown in Figure 4.6 and Figure 4.7. Graphical curves were similar for both groups.

To investigate the effect of phenolin resin in pipe stiffness, two groups were calculated according to ASTM standard, as shown in Table 4.7.

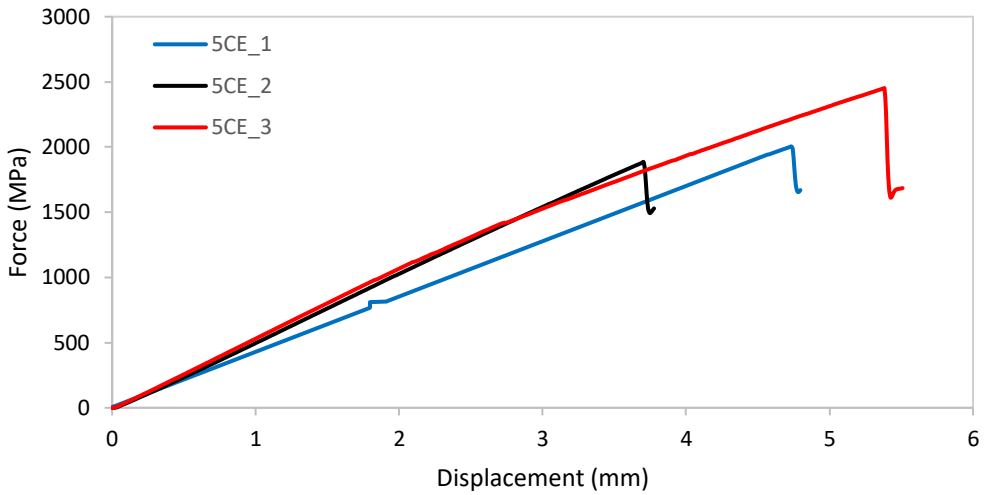


Figure 4.6. Force-Displacement graph of 5-layer carbon epoxy resin samples

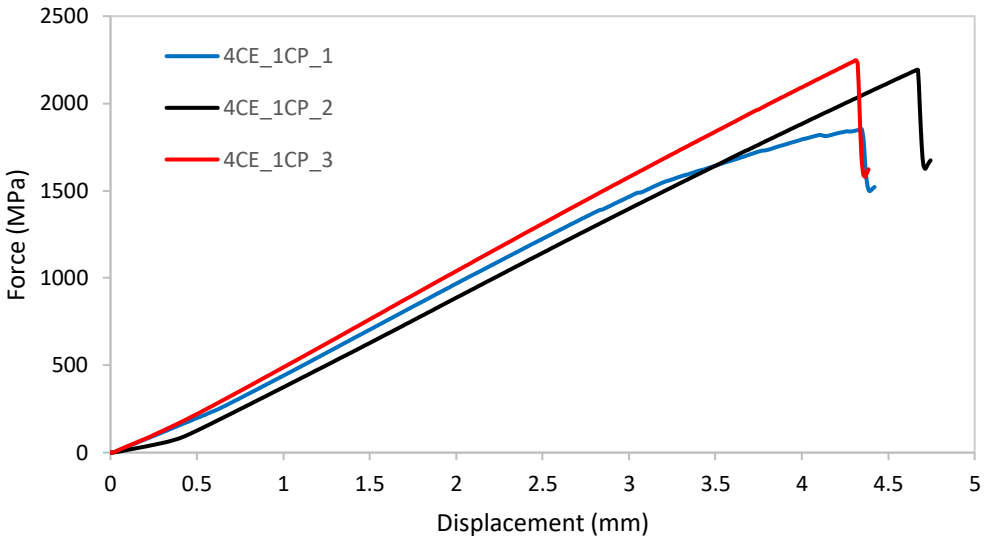


Figure 4.7. Force-Displacement graph of 4-layer carbon epoxy with 1-layer phenolin resin samples

The average pipe stiffness values of composite tubes were calculated as 462.46 ± 43.16 MPa for the 5-layer carbon epoxy group and 472.06 ± 47.57 MPa for the 4-layer carbon epoxy with the 1-layer carbon phenolin resin group.

Table 4.7. Comparison of radial compression test results (average ± standard deviation)

| Sample Name | Pipe Stiffness (N/mm) |
|---|---|
| 5CE | 462.46 ± 43.16 |
| 4CE_1CP | 472.06 ± 47.57 |
| **Difference (%)** | **2.08** |

Results in this study demonstrate that, a significant effect was not observed for pipe stiffness at phenolin resin addition compared to the carbon fiber epoxy resin group. The average stiffness difference was only 2.08%. Failure modes of tube samples after the radial compression test were observed as in Figure 4.8. After the test, the failure behavior of the samples was investigated. Almost no obvious damage was observed, except for the small fiber separations, as shown in Figure 4.9.

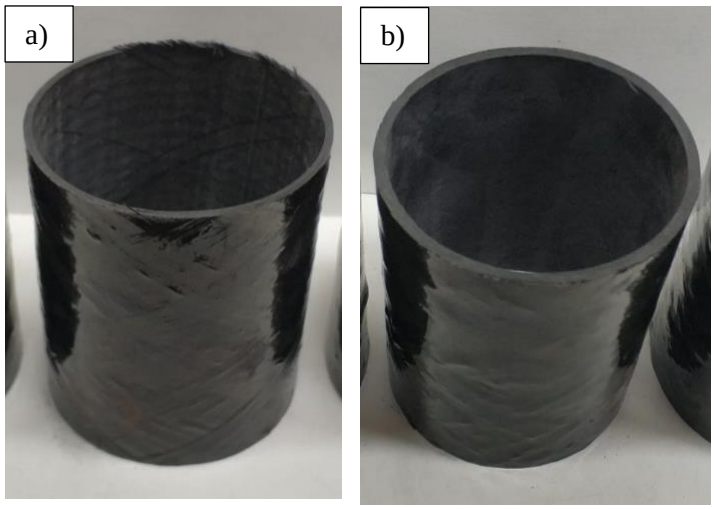


Figure 4.8. Sectioned ring samples after apparent hoop tensile test, a) 5CE, b) 4CE 1P

Figure 4.9. The close-up image of fiber damage after radial compression test

### 4.2.3. Three-Point Bending Test Results

The three-point bending test was applied to the sectioned tube samples to obtain flexural strength, which was calculated for each group with Equation 3.4 according to ASTM D790.

For the calculation, recorded load and displacement data from the test machine were used. Flexural strength results are given for each group in Table 4.8.

Table 4.8. Bending test results of 5-layer carbon epoxy resin tube samples

| Sample Name | Flexural Strength (Mpa) |
|---|---|
| 5CE_1 | 233.09 |
| 5CE_2 | 228.47 |
| 5CE_3 | 239.04 |
| **Average** | **233.54** |
| **St. Dev. (±)** | **5.30** |

Table 4.9. Bending test results of 4-layer carbon epoxy with 1-layer phenolin resin tube samples

| Sample Name | Flexural Strength (Mpa) |
|---|---|
| 4CE_1CP_1 | 248.17 |
| 4CE_1CP_2 | 223.00 |
| 4CE_1CP_3 | 235.84 |
| **Average** | **235.67** |
| **St. Dev. (±)** | **12.59** |

To investigate the effect of phenolin resin in flexural strength, two groups were calculated according to ASTM standard, as shown in Table 4.10.

The average flexural strength values of composite tubes were calculated as 233.54 ± 5.30 MPa for the 5-layer carbon epoxy group and 235.67 ± 12.59 MPa for the 4-layer carbon epoxy with the 1-layer carbon phenolin resin group. Results in this study demonstrate that a significant effect was not observed for pipe stiffness at phenolin resin addition compared to the carbon fiber epoxy resin group. The average stiffness difference was only 0.92%.

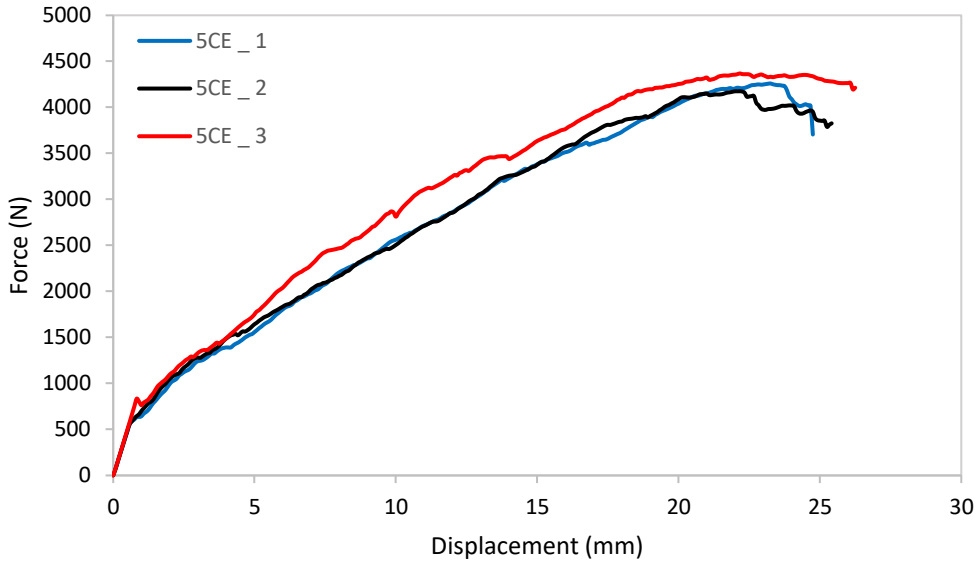


Figure 4.10. Force-Displacement graph of 5-layer carbon epoxy resin samples

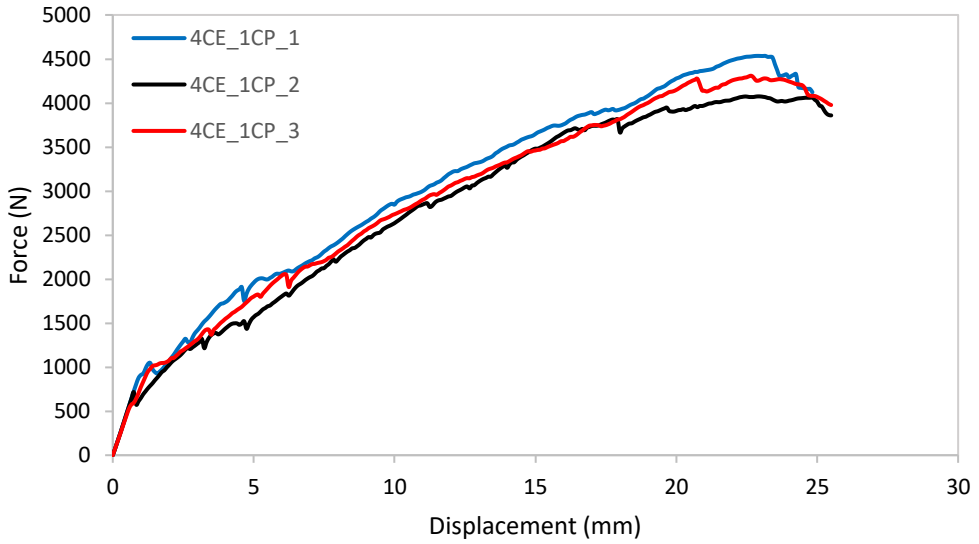


Figure 4.11. Force-Displacement graph of 4-layer carbon epoxy with 1-layer phenolin resin samples

Failure modes of tube samples after the radial compression test were observed as in Figure 4.12. Damage behavior was similar for all samples.

Table 4.10. Comparison of bending test results (average ± standard deviation)

| Sample Name | Flexural Strength (Mpa) |
|---|---|
| 5CE | 233.54 ± 5.30 |
| 4CE_1CP | 235.67 ± 12.59 |
| **Difference (%)** | **0.92** |

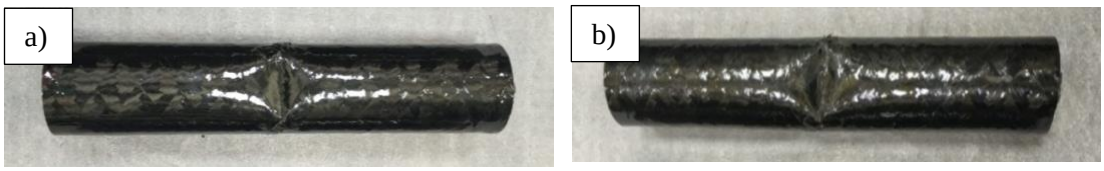


Figure 4.12. Tube samples after 3-point bending test, a) 5CE, b) 4CE 1P

## 4.3. Thermal Properties of Filament Wound Composite Plates

To obtain thermal properties and seek the effects of resin change of configuration, the various thermal tests were prepared and applied. The results are detailed for each test, both numerically and graphically.

### 4.3.1. Thermogravimetric Analysis (TGA) Test Result

The test samples were investigated at 700 $^{o}$C with a 5 $^{o}$C /min step and a 25 $^{o}$C start point of temperature in a nitrogen test atmosphere.

The test results are provided both statistically and graphically by the Center for Materials Research (CMR) within the Izmir Institute of Technology (IZTEC).

The results demonstrate that the thermal behavior of the two groups with the increase in temperature until the end point at 700 $^{o}$C was similar. Although the carbon/phenolin layer showed almost no change in weight until the first onset temperature point at 346.5 $^{o}$C, Additionally, at the carbon/phenolin layer, a 1-step decomposition curve was observed compared to other layer.

The weight change with the increase in temperature was observed graphically, as shown below in Figures 4.13 and 4.14 for both groups.

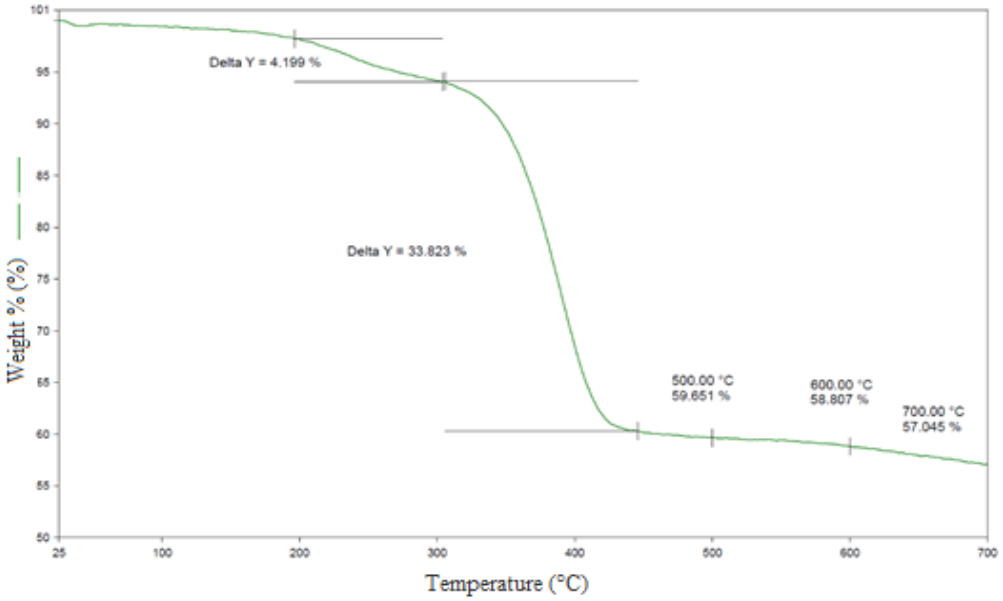


Figure 4.13. TG analysis of carbon/epoxy layer sample

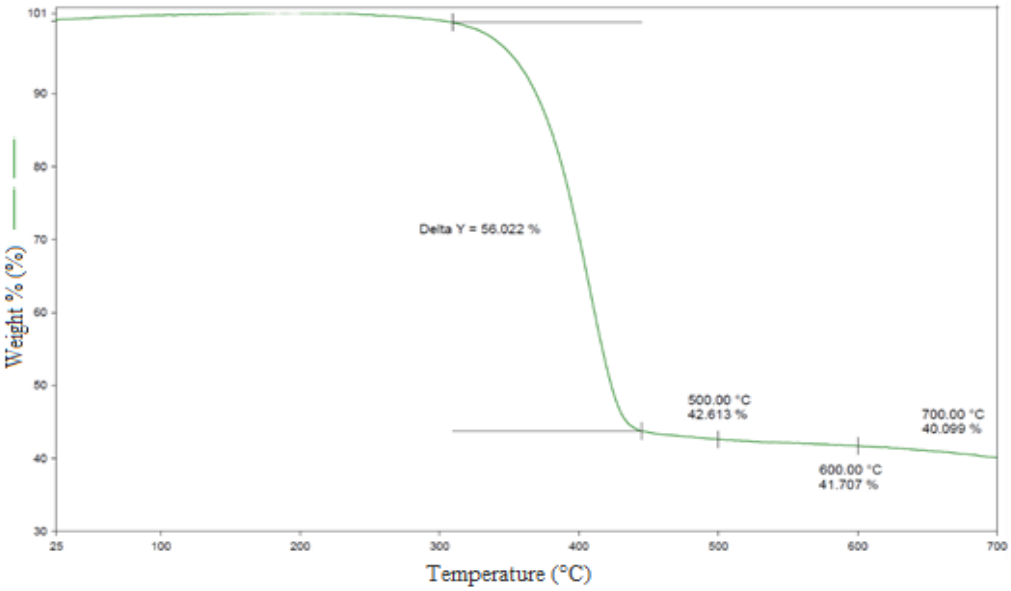


Figure 4.14. TG analysis of carbon/phenolin layer sample

The carbon/epoxy layer showed a 2-step decomposition curve at 230.5 $^{o}$C and 304.2 $^{o}$C, respectively. Decomposition occurred much earlier in the carbon/epoxy layer compared to the carbon/phenolin layer. Therefore, a significant difference can be observed at decomposition phases. But it should be noted that the 5-layer carbon/epoxy sample had more weight percentage at the final temperature point compared to carbon/phenolin sample.

The peak of the first derivative which indicates the point of greatest rate of change on the weight loss curve was also shown in Figures 4.15 and 4.16. Peak temperature of both samples was 401.5 $^{o}$C and 415.7 $^{o}$C, respectively.

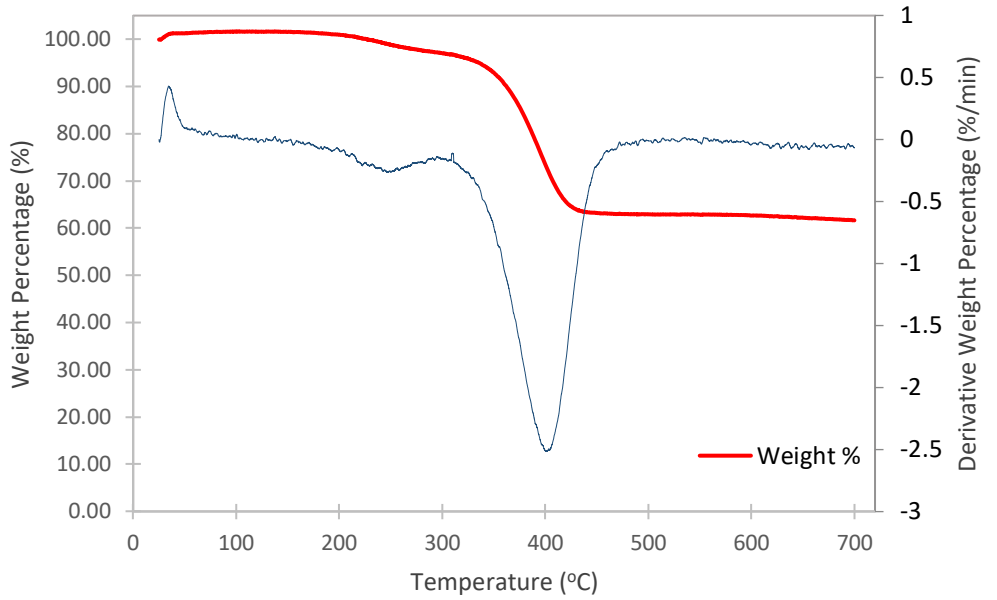


Figure 4.15. 1st Derivative of TGA graph of carbon/epoxy sample

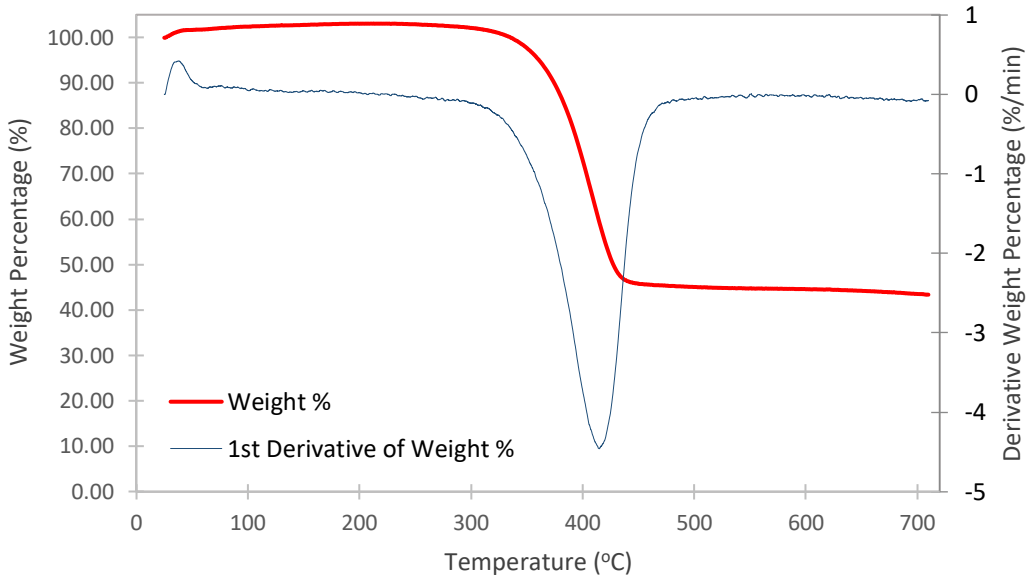


Figure 4.16. 1st Derivative of TGA graph of carbon/phenolic sample

### 4.3.2. Differential Scanning Calorimeter (DSC) Test Result

The test samples were investigated at 500 ºC with a 5 ºC/min increase and a 25 ºC start point. The test results are provided both statistically and graphically by the Geothermal Energy Research and Application Center (GEOCEN) within the Izmir Institute of Technology (IZTEC).

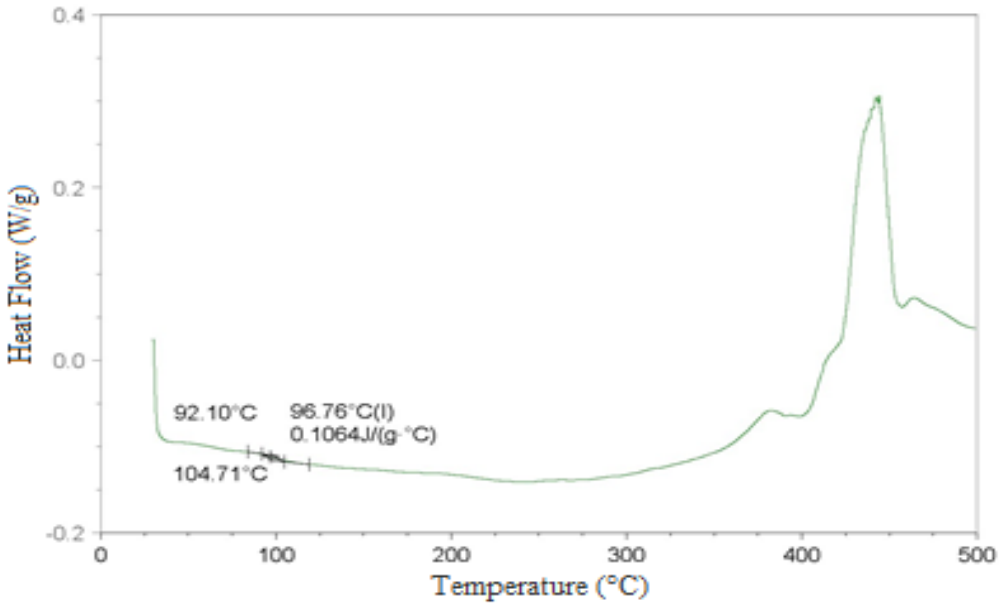


Figure 4.17. DSC analysis of 5-layer carbon/epoxy sample

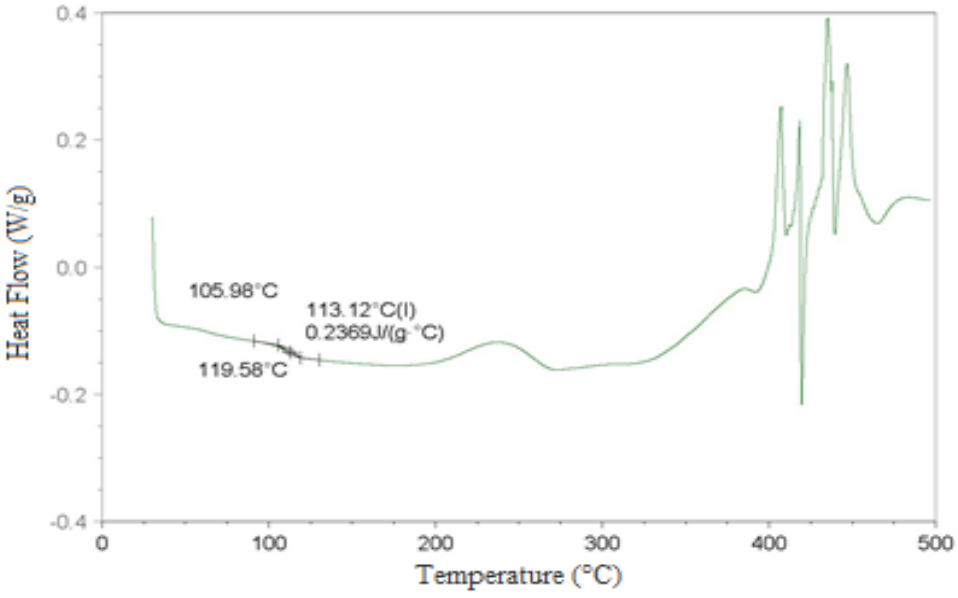


Figure 4.18. DSC analysis of 4-layer carbon/epoxy with 1-layer carbon/phenolin sample

The heat flow with the increase in temperature was observed graphically for both groups, as shown in Figure 4.17 and 4.18. When the results were investigated, the heat flow curve of the two groups was similar. Although the peaks are noisy in the graph, the phenolin sample had better results.

### 4.3.3. Thermal Conductivity Results

The thermal conductivity test could not be performed on sectioned cylindrical samples from composite tubes due to the equipment's inability to analyze cylindrical samples. The test was performed with only plate samples.

The test results were provided statistically by the Geothermal Energy and Research Center (GEOCEN) within the Izmir Institute of Technology (IZTEC), which are shown in Table 4.11.

Table 4.11. Comparison of thermal conductivity test results of plate samples

| Sample Name | Heat Transfer Coefficient (W/mK) |
|---|---|
| 5CE | 3.322 |
| 4CE_1CP | 4.073 |
| **Difference (%)** | **22.61** |

The heat transfer coefficients of the composite tubes were calculated as an estimate with the plate sample results, which are shown in Table 4.12. Therefore, coefficient values may not represent fully correct values for composite tubes.

Table 4.12. Comparison of estimated thermal conductivity result of tube samples

| Sample Name | Heat Transfer Coefficient (W/mK) |
|---|---|
| 5CE | 3.322 |
| 4CE_1CP | 3.449 |
| **Difference (%)** | **3.83** |

The heat transfer coefficient comparison for plate samples was 22.61%. The provided results demonstrate that the coefficient was significantly improved over the

carbon-epoxy plate. In the comparison of the estimated coefficient results of the tubes, the difference was 3.83%, which indicates the difference was not significant.

### 4.3.4. Flammability Results

The flammability test was applied to the sectioned samples from composite tubes to obtain the flame retardancy properties of the tubes. The flash point and burning times were calculated for each group. The results are given for each group in Tables 4.12 and 4.13. It should be noted that the burn damage was not observed inside the tubes.

With the calculation of flammability results, the effect of phenolin addition was calculated, thus a comparison of the two groups was showed in Table 4.15. This table was calculated with the average burning rate and time results of each group.

Table 4.13. Flammability test results of 5-layer carbon/epoxy samples

| Sample Name | Pre-Heat Time (s) | Flash Point Time (s) | Burning Time (s) |
|---|---|---|---|
| CE_30_1 | 30 | 34 | 8.00 |
| CE_30_2 | 30 | 36 | 9.00 |
| CE_30_3 | 30 | 37 | 7.00 |
| **Average** | | **35.67** | **8.00** |
| **St. Dev. (±)** | | **1.53** | **1.00** |

The flash point and burning time results of samples were calculated respectively as 35.67 ±1.53 seconds and 8.00 ±1 seconds for the 5-layer carbon/epoxy group, 42.67 ±1.53 seconds and 3.00 ±1 seconds for the 4-layer carbon/epoxy with 1-layer carbon/phenolin group.

Table 4.14. Flammability test results of 4-layer carbon/epoxy with 1-layer carbon /phenolin samples

| Sample Name | Pre-Heat Time (s) | Flash Point Time (s) | Burning Time (s) |
|---|---|---|---|
| CF_30_1 | 30 | 43 | 3.00 |
| CF_30_2 | 30 | 44 | 4.00 |
| CF_30_3 | 30 | 41 | 2.00 |
| **Average** | | **42.67** | **3.00** |
| **St. Dev. (±)** | | **1.53** | **1.00** |

Results in this study demonstrate that there was a significant effect on flame retardancy properties with phenolin resin addition compared to the carbon/epoxy group.

Table 4.15. Comparison of flammability test results (average ± standard deviation)

| Sample Name | Flash Point Time (s) | Burning Time (s) |
|---|---|---|
| CE 30 | 35.67 ±1.53 | 8.00 ±1 |
| CF 30 | 42.67 ±1.53 | 3.00 ±1 |
| **Difference (%)** | **19.63** | **-62.50** |

Figure 4.19. Half tube sample during flammability test

The differences for flash point and burning times were 19.63% and -62.50%, respectively. Similar results were also observed with other tests, both statistically and visually. Burn damage to samples after the flammability tests was observed as in Figures 4.18, 4.19, and 4.20 for all test scenarios. The fire damage behavior for all samples was visible, but minor differences were observed for both groups. The penetration to the inside layers was only observed with the 600-second heating tests.

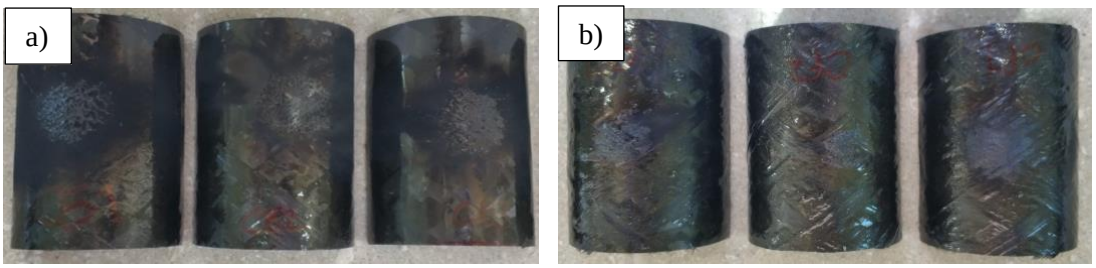


Figure 4.20. Half tube 30-second pre-heat samples after the test, a) 5CE, b) 4CE 1P

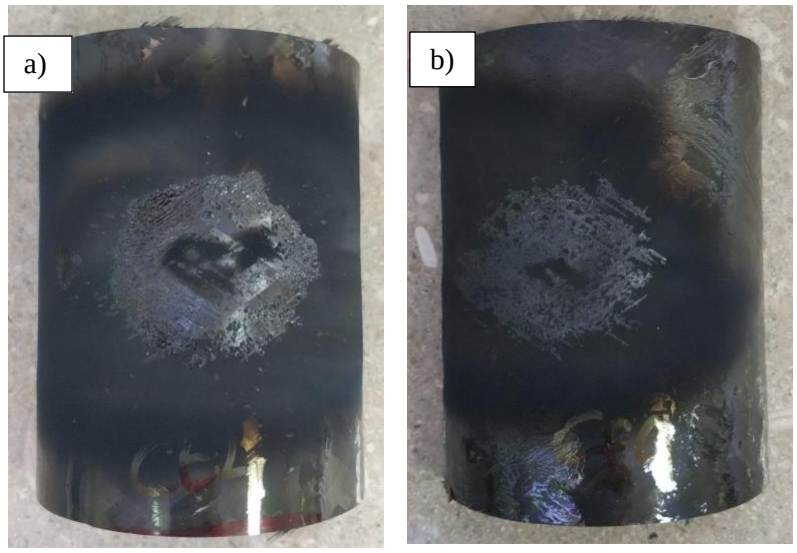


Figure 4.21. Half tube 60-second pre-heat samples after the test, a) 5CE, b) 4CE 1P

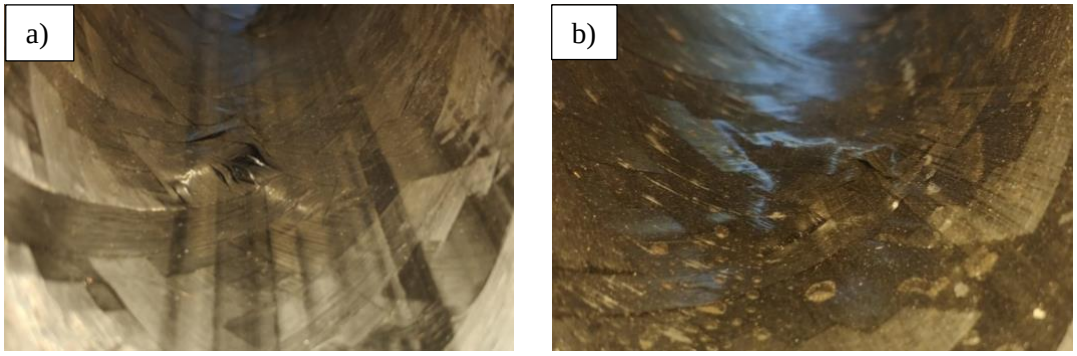


Figure 4.22. Half tube 600-second pre-heat samples after the test, a) 5CE, b) 4CE 1P

# CHAPTER 5

# CONCLUSION

The aim of this study was to investigate the effects of phenolin resin on carbon fiber filament-wound composite tubes. Due to limitations in equipment and phenolin resin properties, the tests were observed for only two configurations of composite tubes. Therefore, the effects of only one (outer) layer of phenolin resin were investigated for thermal and mechanical properties.

The difficulties encountered in this study were related to the capabilities of manufacturing and testing. For the test capabilities, thermal investigations were limited, but all the available procedures were investigated. For the manufacturing aspect, it was due to the material and equipment. Compared to epoxy resin, the phenolin resin cured quickly. Therefore, the reduction of the viscosity of phenolin resin was required with heating. But, due to the lack of heating capabilities of the equipment in the wrapping process, this was not possible for the entire duration of the process. When full phenolin resin stacking manufacturing was experimented with, the first inner layer was wet enough for the next layer's wrapping. However, because the phenolin resin curing had already begun in the resin bath and over the wet fibers, the application of other layers was corrupted, and the fibers were damaged. Improvised solutions for this situation were evaluated, but the results were not satisfying. Therefore, only the 1-layer phenolin resin, which was the outer layer of the tube, was applied over the 4-layer carbon fiber epoxy resin tube. When it was decided that the final production was satisfactory for the research, the study proceeded to the next step.

The comparison between numerical and graphical outcomes demonstrates that no notable or advantageous change was observed in mechanical properties due to the slight difference in values between the test results. But the thermal test results demonstrated that phenolin addition had a significant effect as an improvement on the thermal properties.

The mechanical test results were calculated as follows: For the apparent hoop tensile test, the difference in tensile strength was +0.47%. For the radial compression test, the difference in pipe stiffness results was +2.08%. For the three-point bending test, the comparison of the flexural strength results was +0.92%. The mechanical tests were also

investigated graphically, which indicates that the force-displacement curves were similar for both groups.

The thermal test results were calculated as follows: For the thermal conductivity test, the coefficient differences were 22.61% for plate samples and 3.83% for estimated tube samples. For the flammability test, the difference of flash point and burning time results of samples were 35.67 ±1.53 seconds and 8.00 ±1 seconds for the 5-layer carbon/epoxy group, 42.67 ±1.53 seconds and 3.00 ±1 seconds for the 4-layer carbon/epoxy with 1-layer carbon/phenolin group, respectively. The TGA and DSC results have similar curves, which indicates the behavior of each group was the same under the heating atmosphere. In the TGA test, the weight decreased with similar curves in both groups with the increased temperature. But the first onset temperature point occurred at 346.5 $^{o}$C. For the carbon/phenolin layer, a 1-step decomposition curve was observed compared to the other layer. The carbon/epoxy layer showed a 2-step decomposition curve at 230.5 $^{o}$C and 304.2 $^{o}$C, respectively. Decomposition occurred much earlier in the carbon/epoxy layer compared to the carbon/phenolin layer. DSC test graphical results also indicated the thermal improvement of the structure with phenolin layer addition.

The failure behaviors of both mechanical and thermal experiments were also examined visually during and after the experiments. With the examination of each sample, no significant difference was observed in failure behaviors.

This study also demonstrated that thermal enhancement is possible with the addition of phenolin resin layers without any significant effect on the mechanical properties. Therefore, the phenolin-resin-modified composite filament-wound tubes can be used in applications requiring improved thermal properties.

Considering that only one (outer) layer of the phenolin resin effect was investigated, additional research using various configurations may provide more reliable and different outcomes.

# REFERENCES


[1] Martin, J. W. 2016. “Composite materials.” *Materials for Engineering Chapter-6*: 185-215. doi:10.1533/9781845691608.2.185

[2] Tripaldi, L. 2022. ”Discovering Advanced Composites: How A New Generation of Composite Materials Is Revolutionizing Engineering.” wevolver.com/article/discovering-advanced-composites-how-a-new generation of-composite-materials-is-revolutionizing-engineering

[3] Hasan, Z. 2020. “Composite materials.” *Tooling for Composite Aerospace Structures Chapter-2*: 21–48. doi:10.1016/b978-0-12-819957-2.00002-x

[4] Azeem, Mohammad, Hamdan Haji Ya, Mohammad Azad Alam, Mukesh Kumar, Paweł Stabla, Michał Smolnicki, Lokman Gemi, Rehan Khan, Tauseef Ahmed, Quanjin Ma, Md Rehan Sadique, Ainul Akmar Mokhtar and Mazli Mustapha. 2022. “Application of Filament Winding Technology in Composite Pressure Vessels and Challenges: A Review.” *Journal of Energy Storage*. doi.org/10.1016/j.est.2021.103468

[5] Addcomposites. 2023. “Winding the Future: An Exploration of Filament Winding Applications.” addcomposites.com/post/winding-the-future-an-exploration-of-filament-winding-applications

[6] Bodea, S, Christoph Zechmeister, Niccolo Dambrosio, Moritz Dörstelmann and Achim Menges. 2021. “Robotic Coreless Filament Winding for Hyperboloid Tubular Composite Components in Construction.” *Automation in Construction.* doi.org/10.1016/j.autcon.2021.103649

[7] Cadfil Software. “Filament Winding Overview.” cadfil.com/filamentwinding.html

[8] Ma, Quanjin, M. R. M, Rejab, Idris Mat Sahat, M. Amiruddin, Dandi Bachtiar, Januar Parlaungan Siregar and Mohd Irman Ibrahim. 2018. “Design of Portable 3-Axis Filament Winding Machine with Inexpensive Control System.” *Journal of Mechanical Engineering and Sciences*. doi:10.15282/jmes.12.1.2018.15.0309

[9] Addcomposites. 2022 “What is Filament Winding Process.” addcomposites.com/post/filament-winding

[10] Corvus. 2022. “Composite Manufacturing Processes.” corvuscomposites.com/post/composite-manufacturing-processes

[11] Krishnan, Pranesh, M.S. Abdul Majid, M. Afendi, A.G. Gibson, H.F.A. Marzuki. 2015. “Effects of Winding Angle on The Behaviour of Glass/Epoxy Pipes Under Multiaxial Cyclic Loading.” *Materials & Design*: 196-206. doi.org/10.1016/j.matdes.2015.08.153

[12] Almeida Jr, José Humberto S, Marcelo L. Ribeiro, Volnei Tita and Sandro C. Amico. 2015. "Stacking Sequence Optimization in Composite Tubes Under Internal Pressure Based on Genetic Algorithm Accounting for Progressive Damage." *Composite Structures*: 20-26. doi.org/10.1016/j.compstruct.2017.07.054

[13] Kaynak, Cevdet, E. Salim Erdiller, Levend Parnas and Fikret Senel. 2005. "Use of Split-Disk Tests for The Process Parameters Of Filament Wound Epoxy Composite Tubes." *Polymer Testing*: 648-655. doi.org/10.1016/j.polymertesting.2005.03.012

[14] Morozov, E. V. 2005. "The Effect of Filament-Winding Mosaic Patterns on The Strength." *Composite Structures*: 123-129. doi.org/10.1016/j.compstruct.2006.06.018

[15] Uddin, Md. Sayem, Evgeny V. Morozov, Krishnakumar Shankar. 2014. "The Effect of Filament Winding Mosaic Pattern on The Stress State of Filament Wound Composite Flywheel Disk." *Composite Structures*: *260-275.* doi.org/10.1016/j.compstruct.2013.07.004

[16] Cui, Zhengliang, Qiang Liu, Yubo Sun and Qing Li. 2020. "On Crushing Responses of Filament Winding CFRP/Aluminum and GFRP/CFRP/Aluminum Hybrid Structures." *Composites Part B.* doi.org/10.1016/j.compositesb.2020.108341

[17] Ma, Yan, Toshi Sugahara, Yuqiu Yang and Hiroyuki Hamada. 2015. "A Study on The Energy Absorption Properties of Carbon/Aramid Fiber Filament Winding Composite Tube." *Composite Structures*: 301-311. doi.org/10.1016/j.compstruct.2014.12.067

[18] Abdallah, Maha Hussein, and Abass Braimah. 2022. "Numerical Design Optimization of The Fiber Orientation Of Glass/Phenolic Composite Tubes Based On Tensile And Radial Compression Tests." *Composite Structures 280*. doi.org/10.1016/j.compstruct.2021.114898

[19] Shrigandhi, Ganesh D, and Basavaraj S. Kothavale. 2021. "Biodegradable Composites for Filament Winding Process." *Materials Today: Proceedings 42*: 2762-2768. doi.org/10.1016/j.matpr.2020.12.718

[20] Frollini, E, C.G. Silva and E.C. Ramires. 2013. "Phenolic Resins as a Matrix Material in Advanced Fiber Reinforced Polymer (FRP) Composites." *Advanced Fibre-Reinforced Polymer (FRP) Composites for Structural Applications*: 7-43. doi.org/10.1533/9780857098641.1.7

[21] Ter Meer. 1874. "Ueber die Verbindungen von Phenol mit Aldehyden."

[22] Baeyer A. 1872. "Ueber die Verbindungen der Aldehyde mit den Phenolen und aromatischen Kohlenwasserstoffen." *Berlin Chems 5*: 1094-1100,

[23] Frollini, Elisabete, Alain Castellan. 2012. "Phenolic Resins and Composites." *Wiley Encyclopedia of Composites*: 2059-2068. doi.org/10.1002/9781118097298.weoc167

[24] Ramalingam T, P. Srinivas Yadav, and S. Bhaskar. 2018. “Shell on Shell Bonding of Composite Heat Shield.” *Materials Today: Proceedings 5*: 27155–27160. doi.org/10.1016/j.matpr.2018.09.025

[25] Dong, Wencai, Chonggao Bao, Wenqi Lu, Rongzhen Liu, Haiqiang Ma, Shijia Li and Kun Sun. 2023. “Fabrication of A Continuous Carbon Fiber-Reinforced Phenolic Resin Composites Via In Situ-Curing 3D Printing Technology.” *Composites Communications 38.* doi.org/10.1016/j.coco.2023.101497

[26] Hu, Honglin, Wei Wang, Liqin Jiang, Liang Liu, Ying Zhang, Yunhua Yang, and Jinming Wang. 2022. “Curing Mechanism of Resole Phenolic Resin Based on Variable Temperature FTIR Spectra and Thermogravimetry-Mass Spectrometry.” *Polymers and Polymer Composites 30*: 1-11. doi.org/10.1177/09673911221102114

[27] Azevedo, Cristiano B. de, Frederico Eggers, José H. S. Almeida Jr. and Sandro C. Amico. 2018. “Effect of The Filament Winding Pattern Modeling on The Axial Compression of Cylindrical Shells.“ *Brazilian Conference on Composite Materials*. doi.org/10.21452/bccm4.2018.09.05

[28] Stabla, Paweł, Marek Lubecki, and Michał Smolnicki. 2022. “The Effect of Mosaic Pattern and Winding Angle on Radially Compressed Filament-Wound CFRP Composite Tubes.” *Composite Structures-292*. doi.org/10.1016/j.compstruct.2022.115644

[29] Rajisha, K.R, B. Deepa, L.A. Pothan, and S. Thomas. 2011. “Thermomechanical and Spectroscopic Characterization of Natural Fibre Composites.” *Interface Engineering of Natural Fibre Composites for Maximum Performance*: 241-274. doi.org/10.1533/9780857092281.2.241

[30] Früh, Nikolas, and Jan Knippers. 2021. “Multi-Stage Filament Winding: Integrative Design and Fabrication Method for Fibre-Reinforced Composite Components of Complex Geometries.” *Composite Structures-268*. doi.org/10.1016/j.compstruct.2021.113969

[31] Li, Hang, Shinjiro Sueda, John Keyser. 2021. “Computation of Filament Winding Paths with Concavities and Friction.” *Computer-Aided Design-141*. doi.org/10.1016/j.cad.2021.103089

[32] Sun, Guangyong, Dongdong Chen, Guohua Zhu, and Qing Li. 2022. “Lightweight Hybrid Materials and Structures for Energy Absorption: A State-Of-The-Art Review and Outlook.” *Thin-Walled Structures-172*. doi.org/10.1016/j.tws.2021.108760

[33] Hübner, Fabian, Alexander Brückner, Tobias Dickhut, Volker Altstädt, Agustín Rios de Anda, and Holger Ruckdäschel. 2021. “Low Temperature Fatigue Crack Propagation in Toughened Epoxy Resins Aimed For Filament Winding Of Type V Composite Pressure Vessels.” *Polymer Testing-102*. doi.org/10.1016/j.polymertesting.2021.107323

[34] Wang, Qi, Tong Li, Bo Wang, Changzhi Liu, Qizhong Huang, and Mingfa Ren. 2020. “Prediction of Void Growth and Fiber Volume Fraction Based on Filament Winding Process Mechanics.” *Composite Structures-246*. doi.org/10.1016/j.compstruct.2020.112432

[35] Chang, Yipeng, Weidong Wen, Yiming Xu, Haitao Cui, and Ying Xu. 2022. “Quasi-Static Mechanical Behavior of Filament Wound Composite Thin-Walled Tubes: Tension, Torsion, And Multi-Axial Loading.” *Thin-Walled Structures-177*. doi.org/10.1016/j.tws.2022.109361

[36] Gemi, Lokman, Uğur Köklü, Şakir Yazman, and Sezer Morkavuk. 2020. “The Effects of Stacking Sequence On Drilling Machinability of Filament Wound Hybrid Composite Pipes: Part-1 Mechanical Characterization and Drilling Tests.” *Composites Part B: Engineering-186*. doi.org/10.1016/j.compositesb.2020.107787

[37] Gemi, Lokman, Sezer Morkavuk, Uğur Köklü, and Şakir Yazman. 2020. “The Effects of Stacking Sequence On Drilling Machinability of Filament Wound Hybrid Composite Pipes: Part-2 Damage Analysis and Surface Quality.” *Composites Part B: Engineering-235.* doi.org/10.1016/j.compstruct.2019.111737

[38] Vargas-Rojas, Erik. 2022. “Prescriptive Comprehensive Approach for The Engineering of Products Made with Composites Centered on The Manufacturing Process and Structured Design Methods: Review Study Performed On Filament Winding.” *Composites Part B: Engineering-243.* doi.org/10.1016/j.compositesb.2022.110093